N-linked glycosylation and phosphorylation; what determines legumain localization and activation?

Ingrid Damgaard

Thesis for Master of Pharmacy

Department of Pharmaceutical Bioscience,
Scholl of Pharmacy,
The Faculty of Mathematics and Natural Sciences,
University of Oslo

May 2014

N-linked glycosylation and phosphorylation; what determines legumain localization and activation?

Ingrid Damgaard

Thesis for Master of Pharmacy

Supervisors:

Postdoc Mads Haugland Haugen

Professor Rigmor Solberg

Professor Harald Thideman Johansen

© Ingrid Damgaard

2014

N-linked glycosylation and phosphorylation; what determines protein localization and activation?

Ingrid Damgaard

http://www.duo.uio.no/

Press: Reprosentralen, University of Oslo

Acknowledgments

The present work was performed at the Department of Tumor Biology, Institute for Cancer Research, The Norwegian Radium Hospital, Oslo University Hospital in collaboration with the university of Oslo in the period August 2013 to May 2014.

First of all, I would like to thank my main supervisor Mads Haugland Haugen whose guidance and support has been essential for the completion of this thesis. I have especially valued how you always have taken time to answer my questions even at stressful times. I also admire your broad knowledge and enthusiasm, it has increased my understanding of science. Thank you!

I would also like to thank Gunhild M. Mælandsmo for the opportunity to work on this project and all the members of the Department of Tumor Biology for always being friendly and helpful. A special thanks to Solveig Pettersen for technical support and nice talks, and to the master students (Anna, Marie and Marie) for providing great support and talks.

I am also grateful to my supervisors at the University of Oslo Rigmor Solberg and Harald T. Johansen for journal clubs and constructive comments on this thesis. Thanks to Kristian Prydz for helping me with the sucrose centrifugation and for an educational conversation.

I am especially grateful to my family for giving me advice and “pep talks” throughout the whole period. And finally, I would like to thank Lars Amund for being there the whole time.

Ingrid Damgaard

Oslo, May 2014

Abstract

Metastasis (spread of cancer cells) is the major cause of cancer related deaths. The reason why cancer cells spreads is largely unknown, but proteinases have been suggested to take part in this process. The proteinases have also emerged as promising to utilize in cancer therapy. However, the lack of pre-established knowledge has previously led to failure in clinical trials, e.g. inhibitors against matrix metalloproteinases (MMPs) caused severe side effects in patients. The cysteine proteinase legumain is overexpressed in many solid human tumors, and overexpression is associated with enhanced metastasis. Currently, the knowledge about subcellular localization, trafficking and requirements for legumain activation remains largely unexplored. Known factors that influence the transport and activation of proteins in general are glycosylation and phosphorylation. Both of the aforementioned modifications have been demonstrated on legumain, but the functional role remains unknown.

In this study, we investigated processing and localization of legumain after manipulation of glycosylation and phosphorylation. The colorectal cell lines HCT116 and SW620 were used as cell models. N-linked glycosylation was inhibited by the biochemical tool tunicamycin, whereas phosphorylation was blocked by staurosporine or H7. Legumain expression, processing and distribution were analyzed by immunoblotting and confocal microscopy.

The results have shown that processing of legumain to the mature active form was totally absent after tunicamycin treatment. It was also identified that tunicamycin resulted in a decreased nuclear transport, whereas legumain secretion was apparently not affected. Furthermore, treatment with staurosporine changed the cell morphology, but this was not observed after optimizing the experiment with H7. However, neither staurosporine nor H7 seemed to exert influences on legumain expression or processing.

Overall the results imply that glycosylation, but not phosphorylation, is essential for legumain processing. Furthermore, glycosylation affects legumain transport to the nucleus, but not to the extracellular environment. However, additional research needs to be done to conclude how glycosylation affects intracellular legumain transport.

Table of contents

Abbreviations

AEP	Asparaginyl endopepsidase
ALP	Alkaline phosphatase
ARSB	Arylsulfatase B
Asn	Asparagine
BCA	Bicinchoninic acid
$CaCl_2$	Calcium chloride
CEB	Cytoplasmic extraction buffer
CRC	Colorectal cancer
DAPI	4',6-diamidino-2-phenylindole
ddH_20	Double distilled water
DMSO	Dimethyl sulfoxide
Dol-P	Dolichol phosphatase
DTT	Dithiotreitol
EEA1	Early endosomes antigen 1
Endo H	Endoglycosidase H
FBS	Foetal bovine serum
H7	1-(5-isoquinolinesulfonyl)-2-methylpiperazine
HS	Horse serum
IC_{50}	“Half maximal inhibitory concentration”
kDa	Kilodalton
K_i	“Binding affinity of the inhibitor”
LDS	Lithium dodecyl sulfate
MEB	Membrane extraction buffer
MMP	Matrix metalloproteinase
MTS	3-4,5-dimethylthiazol-2-yl)-5-(3-carboxymethoxyphenyl)-2-(4-sulfophenyl)
N	Asparagine

NEB	Nuclear extraction buffer
PBS	Phosphate-buffered saline
PEB	Pellet extraction buffer
PES	Phenazine etosulfat
PFA	Paraformaldehyde
PKC	Protein kinase C
PNGase F	Peptide –N-glycosidase F
PSK	Protein serine/threonine kinase
PTK	Protein tyrosin kinase
PVDF	Polyvinylidene difluoride
RER	Rough endoplasmatic reticulum
rhLeg	Recombinant human prolegumain
RPMI	Roswell Park Memorial Institute medium
S	Serine
SDS	Sodium dodecyl sulfate
SP1	Specificity protein 1
T	Threonine
TBST	Tris-Buffered Saline with Tween 20
Y	Tyrosine

1 Introduction

1.1 General principles of cancer

Cancer is a collective term of a large group of genetic conditions initiated by uncontrolled cell growth. Normally, there is a balance between genes that promote- and suppress cell proliferation. However, some of these genes can be subjected to mutations which cause uncontrolled cell multiplication, and the cells lose their original functions. As the division continues there will be an accumulation of cancer cells in a limited area, giving rise to a primary tumor (Norwegian Electronic Legehåndbok, 2014).

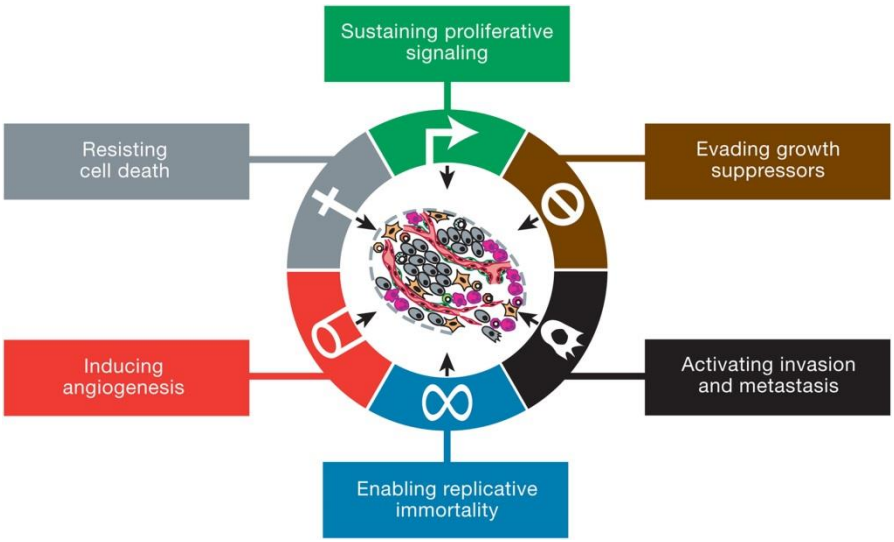

Figure 1.1: Hallmarks of cancer. The figure illustrates the six acquired hallmarks during cancer development (Hanahan *et al.*, 2011).

Cancer evolves progressively, and the complexity of neoplastic diseases may be summarized by six acquired biological capabilities, also known as hallmarks of cancer (Fig. 1.1). These capabilities, that distinguish cancer from normal cells, includes sustaining proliferative signaling, evading growth suppressors, resisting cell death, enabling replicative immorality, inducing angiogenesis and activating invasion and metastasis (Hanahan *et al.*, 2011).

1.2 Invasion and metastasis

Metastasis is the major cause of cancer-related deaths, and constitutes a major problem for cancer therapy. Metastasis is a multistage process, commonly termed the invasion-metastasis cascade, during which cells spread from the primary tumor via blood and lymphatic vessels to distant anatomical organ sites. Cancer cells that metastasize have undergone a series of genetic alterations, and the process is initiated by local invasion, which is entry of cancer cells from the primary tumor into the adjacent normal tissues (Fig. 1.2). A small proportion of these cells may end up circulating in the blood or lymphatic system. An even smaller fraction of these circulating tumor cells may eventually extravasate at a distant location and start dividing. The end product of the invasion-metastasis cascade is secondary tumors, also known as metastases (Talmadge *et al.*, 2010, Valastyan *et al.*, 2011).

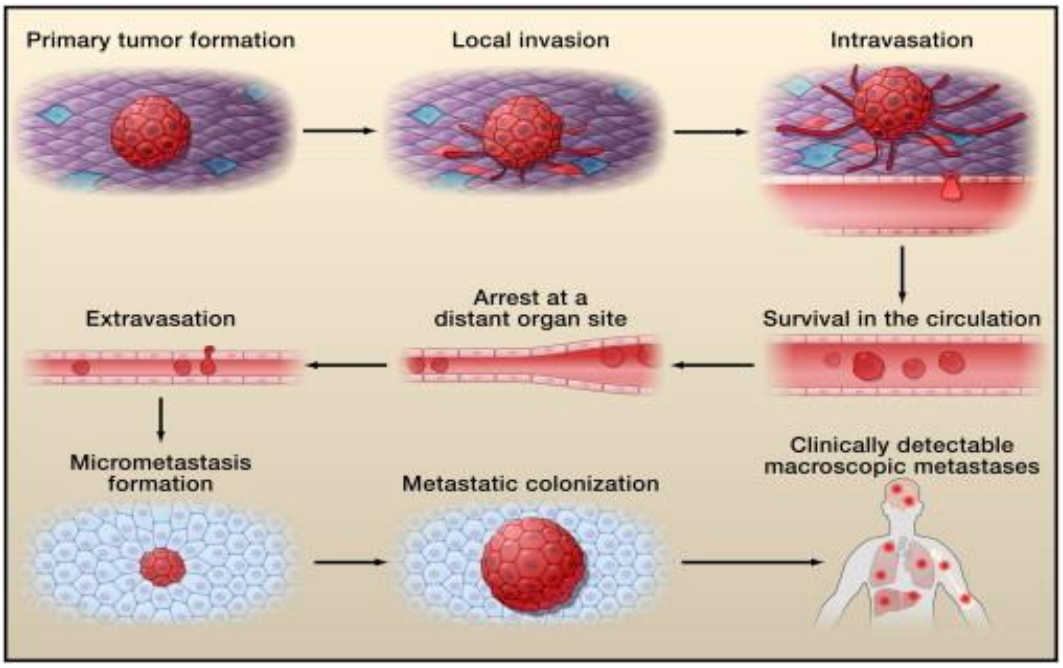

Figure 1.2: The invasion-metastasis cascade. The figure shows the main steps in the formation of metastases (Valastyan *et al.*, 2011).

1.3 Colorectal cancer

1.3.1 Prevalence

Colorectal cancer (CRC) is the third most common cancer worldwide, and is the fourth most frequent cause of cancer death affecting both sexes (Weitz *et al.*, 2005, Ferlay *et al.*, 2010). In

Norway, CRC is the fourth frequent cancer and the second frequent cause of cancer death (both sexes) (Cancer Registry of Norway, 2011).

1.3.2 Pathogenesis and risk factors

Colorectal cancer is a disease of the colon or rectum, and begins in the epithelial cells in the innermost layer (mucosa) of the large intestine. Underneath this mucosa layers lies the submucosa, which contains blood and lymphatic vessels. If the cancer cells invade into the submucosa, it can gain entrance to the blood supply, permitting spread throughout the body (Frayling, 2001, Yeatman, 2001).

The majority of colorectal cancers arise sporadically, and the risk factors involves increasing age, male sex, unhealthy lifestyle, smoking, etc. (Weitz *et al.*, 2005). However, approximately 20 % of CRC patients are estimated to have some component of familiar risk (Lynch *et al.*, 2003).

1.4 Proteinases

Proteinases are specialized enzymes which catalyze the cleavage of proteins by hydrolysis. In the literature, proteinases are also known as proteases, proteolytic enzymes and peptidases (Barrett, 2001, Barrett *et al.*, 2013). More than 600 proteinases have been identified and they are classified based upon their distinct catalytic mechanism for substrate hydrolysis, into aspartic, cysteine, glutamic, metallo, threonine and serine proteinases. Proteinases can be subdivided into endopeptidases or exopeptidases, reflecting their cleaving position in the polypeptide chain. Endopeptidases cleave internal bonds in the polypeptide, while exopeptidases act near the N- or C-terminal end of the polypeptide chain (Chwieralski *et al.*, 2006, Turk, 2006, Barrett *et al.*, 2013). In the modern classification system, MEROPS peptide database, proteinases are dived into families and clans based upon the structural similarities. Individual proteinases are grouped into families on the basis of the similarities in the amino acid sequences. The families, which most likely share a common origin, are further grouped together in a clan (Barrett, 2001, Barrett *et al.*, 2013).

The primary role of proteinases were long considered to be digestion of food and protein turnover. However, proteinases have also been found to be important signal molecules that are involved in numerous vital processes, such as immune responses, cell proliferation, cell

death and DNA replication. Proteinase signaling pathways are strictly regulated, and aberrant regulation of proteinase activity may contribute to pathologies such as cancer (Barrett, 2001, Turk, 2006, López-Otín *et al.*, 2008).

1.5 Legumain

Legumain is a cysteine endopepsidase which belongs to the C13 peptidase family of clan CD (Fig. 1.3) (Rawlings *et al.*, 2014). It was originally discovered and isolated from plants and a blood fluke, before Chen *et al.* described the mammalian version (Chen *et al.*, 1997). Legumain shows strict specificity for hydrolysis of peptide bonds at the C-terminal side (position P1) of asparaginyl in substrates and, to a lesser extent, after aspartic acid at low pH (Chen *et al.*, 1997, Halfon *et al.*, 1998). In the literature, legumain is synonymously termed asparaginyl endopepsidase (AEP), reflecting its strict specificity and function (Li *et al.*, 2003). The proteinase cathepsin B, H and L are examples of substrates that are processed by legumain (Shirahama-Noda *et al.*, 2003), and the most potent endogenous inhibitors are cystatin C (K_i 0.20 nM) and cystatin E/M (K_i 0.0016 nM) (Alvarez-Fernandez *et al.*, 1999). Legumain is primarily localized in the late endosomes and lysosomes, in conjunction with the acidic environment which is considered to be favorable for proteolytic activity (Chen *et al.*, 1998). In addition, proteolytic active legumain has also been observed in the nucleus and prolegumain in the extracellular environment (Haugen *et al.*, 2013).

In non-disease mammalian tissues, legumain is predominantly found in the kidney and placenta. Moreover, legumain expression and enzymatic activity is also detected in the spleen, liver, thymus and testis, although to a lesser extent (Chen *et al.*, 1997, Chen *et al.*, 1998).

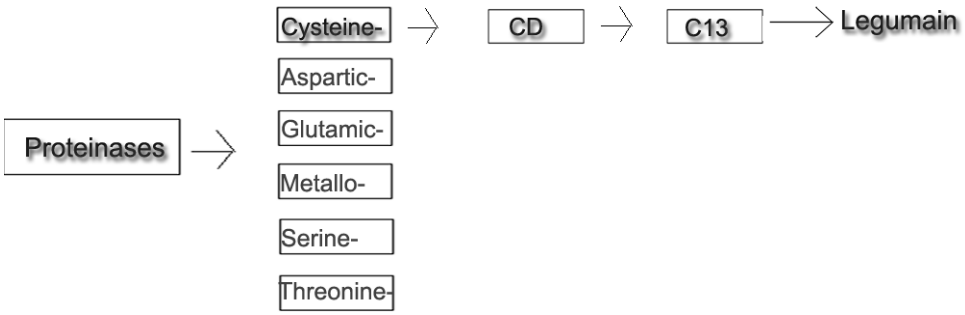

Figure 1.3: Classification of legumain.

1.5.1 Legumain activation

Legumain is translated as an inactive proenzyme of 56 kDa termed prolegumain. How this proteinase itself is activated is not fully characterized, but a multi-step process is thought to involve both autocatalytic processing at different pH thresholds, as well as involvement of other proteinases (Li *et al.*, 2003).

Full length prolegumain of 56 kDa is stable and enzymatically inactive at neutral pH. One theory is that once the pH is lowered below 5.5, an autocatalytic cleavage of the C-terminal domain is initiated, resulting in an inactive intermediate of 47 kDa (Fig. 1.4). A further decrease in pH triggers the release of the N-terminal propeptide and produces an active intermediate of 46 kDa. *In vivo*, the 46 kDa intermediate is further processed to the fully active form of 36 kDa by the involvement of other lysosomal proteinases (Li *et al.*, 2003). Recent results demonstrate that the complex maturation process may be reversed (Zhao *et al.*, 2014).

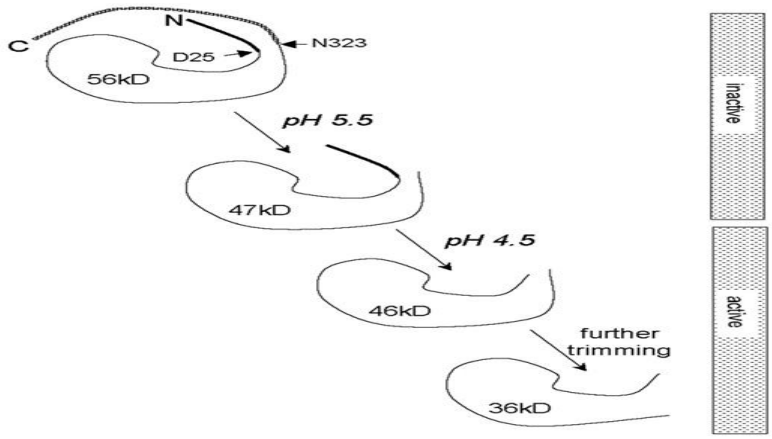

Fig 1.4: Suggested scheme for legumain activation. Upon pH lowering, the inactive proenzyme of 56 kDa is progressively converted to 47 kDa (inactive) and to 46 kDa (active) legumain. *In vivo*, the 46 kDa intermediate is further processed to the fully active form of 36 kDa by other lysosomal proteinases (adapted from (Li *et al.*, 2003)).

1.5.2 Cellular functions of legumain

Legumain is up-regulated in the majority of human solid tumors, such as colorectal, prostate and breast cancers (Liu *et al.*, 2003). In tumor cells, legumain is localized both intracellularly and on the cell surface. Intracellular legumain is predominantly distributed in the membrane-associated vesicles i.e. Golgi, endosomes and lysosomes (Liu *et al.*, 2003, Murthy *et al.*, 2005), nevertheless, the proteinase does not seem to be exclusively confined to these subcellular structures. Most recently, Haugen *et al.* demonstrated legumain expression and proteolytic activity in the nucleus of CRC cells. However, the biological function of active legumain in the nucleus has not yet been elucidated (Haugen *et al.*, 2013).

Legumain has been shown to facilitate cell migration, and overexpression in tumors is associated with enhanced invasion and metastasis (Liu *et al.*, 2003). These properties might be in connection with legumain being shown to activate the matrix metalloproteinase (MMP) progelatinase A in cultured cells (Chen *et al.*, 2001). It has been hypothesized that tumors that express high levels of legumain would display a more aggressive behavior and result in a poor prognosis, which has been confirmed in CRC (Liu *et al.*, 2003, Murthy *et al.*, 2005).

Other known important cellular functions of legumain is within the immune system where it has been shown to process microbial antigens for MHC class II presentation, and assist in proteolytic maturation of Toll-like receptor 9 (Manoury *et al.*, 1998, Sepulveda *et al.*, 2009).

Legumain has also been associated with atherosclerosis (Clerin *et al.*, 2008), stroke (Liu *et al.*, 2008) and to be involved in bone resorption as it inhibits osteoclast formation (Choi *et al.*, 1999).

1.6 Utilizing proteinases in prodrug activation in cancer therapy

Current compounds used in cancer medicine are generally not very specific and cause undesirable cytotoxicity to normal cells. A promising approach to increase selectivity is to exploit physiological conditions of the target tissue that differs greatly from that of other tissues. Proteinases are upregulated in many human tumors. The high levels in tumor cells coupled with their ability to cut specific substrates (amino acid sequences) makes proteinases attractive candidates for selective prodrug activation in cancer therapy (Mahato *et al.*, 2011, Choi *et al.*, 2012). Prodrugs are inactive derivatives of active drug molecules that must undergo a conversion *in vivo* to exert their pharmacological effect, e.g. by utilizing proteinases (Huttunen *et al.*, 2011, Choi *et al.*, 2012).

Adcetris ® (brentuximab vedotin) is an example of an approved prodrug against lymphoma, that utilizes the proteinase cathepsin B for activation (Katz *et al.*, 2011). Legumain shows (as previously mentioned) restricted specificity C-terminally to asparagine, and is to date the only known human proteinase with this specificity (Chen *et al.*, 1997, Dando *et al.*, 1999). Because of this strict substrate specificity and high-level expression in many human tumors, legumain represent a highly relevant proteinase which can be utilized for prodrug activation in selective cancer treatment (Liu *et al.*, 2003). It has been done several preclinical studies where high potent chemotherapeutics (e.g. doxorubicin, auristatin, dolastatin) have been masked with a peptide that is cleaved in the presence of legumain (Fig. 1.5) (Liu *et al.*, 2003, Bajjuri *et al.*, 2011, Liu *et al.*, 2012). However, former unsuccessful clinical trials have shown that detailed knowledge about proteinases, such as function and localization, are essential for development of proteinase-activated prodrugs (Turk, 2006, Choi *et al.*, 2012).

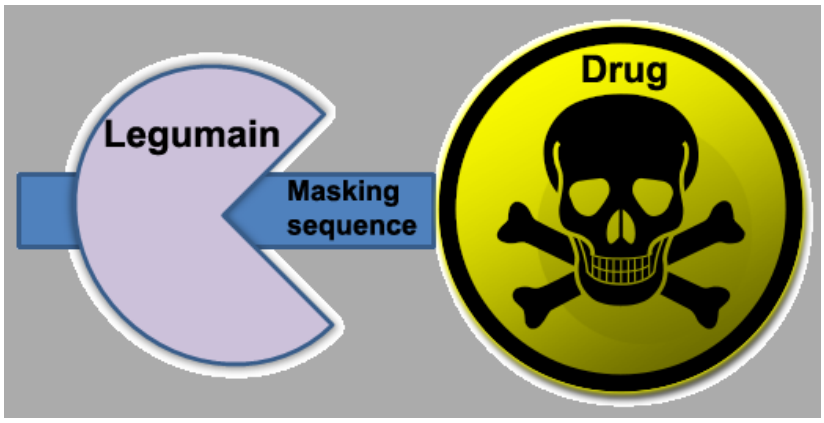

Figure 1.5: A proteinase-activated prodrug strategy. Incorporating of a legumain masking sequence onto high potent chemotherapeutics is a promising approach to increase the selectivity of cancer therapy.

1.7 Protein modifications

Structural modifications of proteins can occur either during synthesis, cotranslational modifications, or after synthesis, posttranslational modifications (Shandala *et al.*, 2001). Protein modifications have been shown to be essential in cell regulation because they can potentially influence chemical properties, stability, activity and cellular location of proteins. There have been identified over 400 protein modifications, where phosphorylation and glycosylation are among the most common and well-studied (Sparbier *et al.*, 2005, Farley *et al.*, 2009).

1.8 Protein glycosylation

Protein glycosylation, which is covalent attachment of sugar moieties to polypeptides, is an important posttranslational modification (Shandala *et al.*, 2001). It is estimated that more than half of all mammalian proteins are glycosylated (Apweiler *et al.*, 1999, Zafar *et al.*, 2011). Glycosylation is vital for a wide range of biological processes, and has been shown to affect enzyme activity, protein localization and stability. There are five main types of glycosylation with various carbohydrate structures, but the most abundant are N- or O-linked glycosylation (Ohtsubo *et al.*, 2006, Farley *et al.*, 2009, Zafar *et al.*, 2011).

1.8.1 N-linked protein glycosylation

N-linked glycosylation occurs in the rough endoplasmic reticulum (RER), and involves the attachment of high-mannose oligosaccharide structures to selected asparagine (Asn) residues in the polypeptide backbone (Shandala *et al.*, 2001).

The high mannose oligosaccharide structure, containing a total of 14 sugars, is synthesized by a sequential process. The biosynthesis commences on the cytoplasmic side of the RER and terminates at the lumenal face, giving rise to the final oligosaccharide precursor product $Glc_3Man_9GlcNAc_2$-PP-dolichol. In the lumen of RER, the completed oligosaccharide structure is then transferred *en bloc* to selected Asn residues as nascent proteins are being translocated into the RER (Kornfeld *et al.*, 1985, Shandala *et al.*, 2001). Asparagine acceptors that are glycosylated are always present in the tripeptide sequence N-X-S/T, where N is asparagine, X is any amino acid except proline and S/T are, respectively, serine or threonine. However, the presence of this consensus tripeptide motif appears to be necessary but not sufficient for the protein to serve as an acceptor *in vivo* (Pless *et al.*, 1977, Kornfeld *et al.*, 1985).

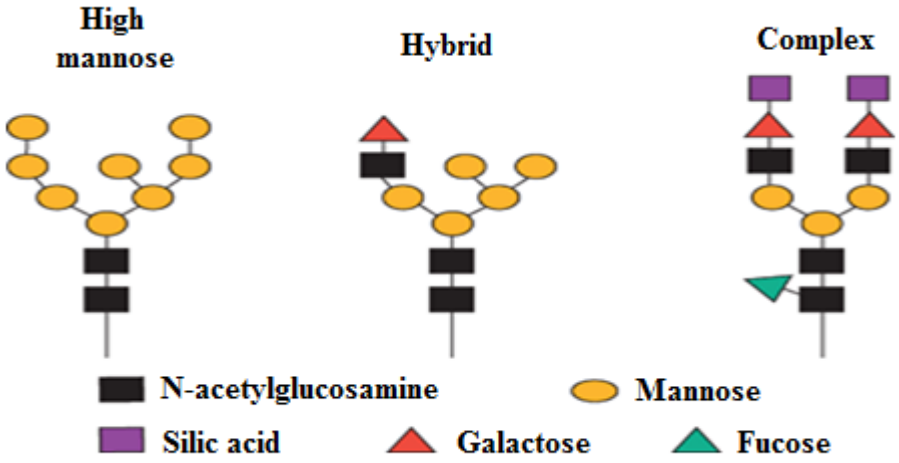

Figure 1.6: Structures of the major types of N-linked oligosaccharides (adapted from (Shandala et al., 2001)).

Once the glycosylation has occurred, the oligosaccharide precursor is subjected to a variety of processing and modifications in the RER and Golgi apparatus. This elaboration of the oligosaccharide leads formation of one of the three main types of N-linked oligosaccharide structure, termed “high mannose”, “hybrid” and “complex” (Fig 1.6) (Kornfeld *et al.*, 1985, Shandala *et al.*, 2001). The potential for diversity in the composition of oligosaccharides that

can be attached to the protein and remodeling of the sugar chain can result in heterogeneity of the end-stage glycoproteins (Shandala *et al.*, 2001, Aebi, 2013).

1.8.2 Legumain and N-linked glycosylation

The glycosylation pattern of legumain in two colorectal cells, HCT116 and SW620, has previously been investigated (Haugen *et al.*, Dept. of Tumor Biology, Oslo University Hospital), and the protein band size of the unglycosylated forms of legumain was observed (Fig. 1.7 B). The CRC cell lines were treated with PNGase F, an enzyme which removes N-linked glycosylation (see chapter 1.8.4), and analyzed by gel electrophoresis (4-12 % gradient gel) and immunoblotting of legumain. First, the immunoblot demonstrated a noticeable mass shift in both cell lines after PNGase F treatment from 56 kDa to approximately 47 kDa for the proform and from 36 kDa to 28 kDa for the mature active form of legumain. This indicates that legumain is subjected to N-linked glycosylation (Fig. 1.7). Second, incomplete PNGase F treatment of HCT116 cells gave rise to three distinct bands located below the glycosylated 36 kDa band in the control, which demonstrated that least three of the four potential glycosylation sites in legumain are occupied (Fig. 1.7) (Haugen *et al.*, unpublished data).

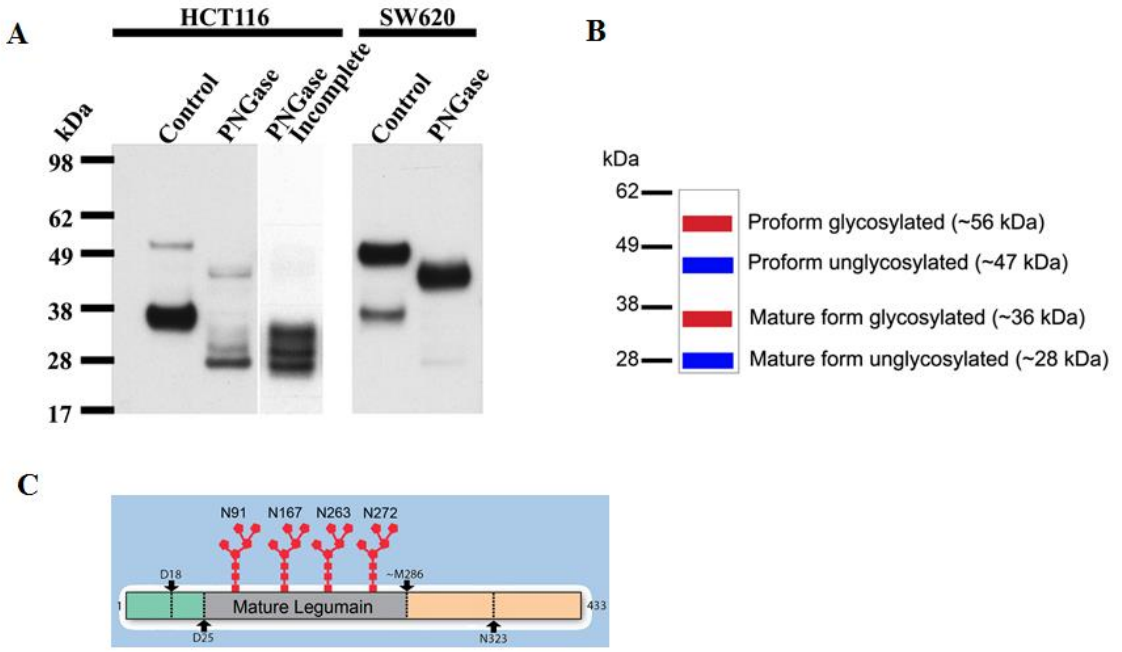

Figure 1.7: N-linked glycosylation of legumain. (A) Legumain expression in HCT116 and SW620 cell lysates when deglycosylated by treatment with PNGase F (Haugen *et al.*, unpublished data). (B) Estimated protein band sizes of the glycosylated and unglycosylated forms of legumain. (C) The potential glycosylation sites (red) on asparagine (N) acceptors in legumain.

1.8.3 Tunicamycin, an inhibitor of N-linked glycosylation

Tunicamycin is a nucleoside antibiotic isolated from *Streptomyces lysosuperificus* (Takatsuki *et al.*, 1971). Tunicamycin specifically inhibits the first step in the biosynthesis of the high mannose oligosaccharide, i.e. the transfer of GlcNac-1-P to the specialized lipid dolichol phosphatase (Dol-P). If this step is inhibited *in vivo*, the oligosaccharide cannot be formed and the glycosylation of a protein is prevented. Moreover, the inhibitory action of tunicamycin seems to be restricted exclusively to the transfer of the GlcNAc moiety, whereas further glycosyl transfer reactions are not affected (Tkacz *et al.*, 1975, Lehle *et al.*, 1976, Heifetz *et al.*, 1979).

Tunicamycin is a powerful experimental tool for studying the role of glycoproteins in a wide range of biological systems (Heifetz *et al.*, 1979). Working as a competitive tight-binding inhibitor, the concentration described to prevent glycosylation varies between 0.1 - 10 µg/ml (Elbein, 1987). The treatment time *in vivo* has been suggested to be 24 hours, which may permit a cell to replace many endogenous glycoproteins with proteins synthesized in the

presence of tunicamycin. However, for proteins with a slower or faster turnover than average, longer or shorter incubation times may be appropriate (Powell, 2001).There are several cautions that should be taken into account using tunicamycin in biochemical studies, especially its toxic effect. Tunicamycin can inhibit cell division *in vitro* by arrest cells in G_1 of the cell cycle. However, not all cell systems are sensitive (Savage *et al.*, 1983, Elbein, 1987).

1.8.4 PNGase F and Endo H

Peptide -N-glycosidase F (PNGase F) and endoglycosidase H (Endo H) are enzymes which are used as biochemical research tools for protein deglycosylation (Kuhn *et al.*, 1994, O'Neill, 1996). PNGase F removes all types of oligosaccharides (high mannose, hybrid or complex) (Fig. 1.6) from proteins. This enzyme cleaves the bonds between the innermost oligosaccharide and the amino acid sequence, making the protein of interest fully deglycosylated (Kuhn *et al.*, 1994). Endo H is a highly specific endoglycosidase, which cleaves within the core of the oligosaccharide and removes primarily high mannose oligosaccharides, and to some extent, hybrid oligosaccharides from proteins. This enzyme can be used to determine the type of N-linked glycosylation (O'Neill, 1996).

1.9 Protein phosphorylation

Protein phosphorylation is a reversible protein modification, and involves the covalent attachment of a phosphate group to an amino acid in the target protein. The amino acid residue(s) to which the phosphate group is transferred is usually a serine, threonine or tyrosine, but histidine or lysine residues have also been found to be phosphorylated. Protein phosphorylation and dephosphorylation are catalyzed by protein kinases and protein phosphatases, respectively (Krebs *et al.*, 1979, Hunter, 1989, Graves *et al.*, 1999). It has been estimated that 30 % of the human proteome is phosphorylated, and the reversible process has been shown to have a regulatory role in a multitude of cellular processes such as proliferation, migration, protein transcription and apoptosis (Cohen, 2001, White, 2008, Farley *et al.*, 2009).

1.9.1 Legumain and phosphorylation

Legumain phosphorylation has recently been investigated in the colorectal cell line HCT116 (Haugen *et al.*, Dept. of Tumor Biology, Oslo University Hospital). The cell line was treated with alkaline phosphatase (ALP), which removes phosphate groups from proteins, and analyzed by 2D gel electrophoresis and immunoblotting of legumain. In comparison to the control lysates, removal of the phosphate group using ALP resulted in a visible shift towards the anionic end (Fig. 1.8 A). This indicates that the charge of the protein has been modified, and thus that legumain has been de-phosphorylated. *In silico* analysis (computer simulation) predicted that there were totally 15 potential phosphorylation sites at the serine (S), threonine (T) and tyrosine (Y) residues in legumain (Fig. 1.8 B) (Blom *et al.*, 1999). However, which of the predicted phosphorylation sites that are occupied or the function of these phosphorylations have not been elucidated (Haugen *et al.*, unpublished data).

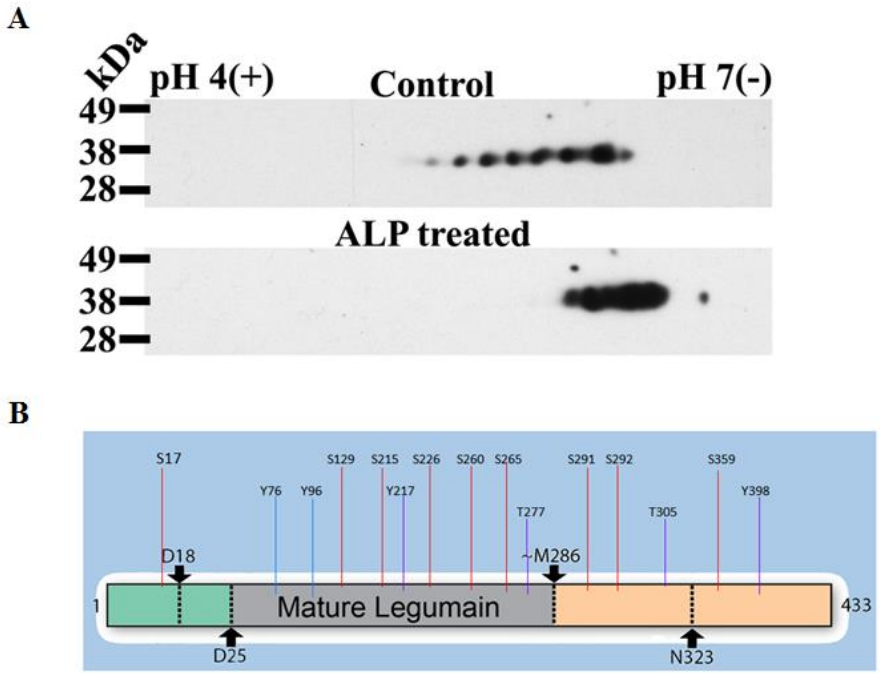

Figure 1.8: Phosphorylation of legumain. (A) The cell lysates were treated with (lower panel) or without (upper panel) ALP and analyzed by 2D gel electrophoresis and immunoblotting of legumain. The protein pattern in the cell lysate treated with ALP compared to the control showed a clear shift towards the anionic end, which demonstrated removal of phosphate groups on legumain (Haugen *et al.*, unpublished data). (B) Predicted phosphorylation sites on the serine (S), threonine (T) and tyrosine (Y) amino acid sequences in legumain using NetPhos 2.0 method, which have a sensitivity in the range from 69-96 % (Blom *et al.*, 1999).

1.9.2 Protein kinases

The protein kinases make up a large family of homologous protein which perform protein phosphorylation (Hanks *et al.*, 1995). As phosphorylation has a regulatory role in many cellular processes, it has been a growing interest in developing specific inhibitors of protein kinases for clinical use (Cohen, 2002).

Protein kinases are generally classified into two broad classes, protein serine/threonine kinases (PSK) and protein tyrosine kinases (PTK), on the basis of the amino acids phosphorylated in their protein substrates. Protein kinases can further be grouped into subfamilies based on overall similarities in the catalytic domain sequences. The individual members are grouped together primary on the basis of their similar catalytic domain sequence. The protein kinase C (PKC) referred to in chapter 1.9.3 and 1.9.4 is member of the protein serine/threonine kinases (PSK) (Hanks, 1991, Hanks *et al.*, 1995).

1.9.3 Staurosporine, a broad spectrum protein kinase inhibitor

Staurosporine is an alkaloid isolated from *Streoptomyces staurosporeus* (Omura *et al.*, 1977). Staurosporine is a cell permeable compound and is potent inhibitor of protein kinase C (PKC) with an IC_{50} value in the nanomolar range (Tamaoki *et al.*, 1986). In addition, staurosporine is also an inhibitor of a variety of other protein kinases *in vitro* in a rather nonspecific manner (Ruegg *et al.*, 1989). Staurosporine has shown to exhibit strong cytotoxic effects at micromolar concentrations, and to induce apoptosis in a variety of cells using concentrations in a wide range (100 nmol/L-100 µmol/L) (Tamaoki *et al.*, 1986, Zhang *et al.*, 2003).

1.9.4 H7, a narrow spectrum protein kinase inhibitor

H7 (1-(5-isoquinolinesulfonyl)-2-methylpiperazine) is a reversible and selective protein kinase inhibitor. H7 has highest potency towards protein kinase C (PKC), compared to other kinases, with a K_i value of 6 µM. H7 is a synthetic compound, and serve as a useful pharmacological tool for elucidation of protein phosphorylation (Hidaka *et al.*, 1984).

2 Aims of the present study

The aim of the present project is to investigate whether pharmacological manipulation of legumain modifications like phosphorylation and glycosylation will influence legumain activation and subcellular transport. To test these hypotheses legumain expression and distribution in the CRC cell lines HCT116 and SW620 cells will be characterized after treatment with tunicamycin (an inhibitor of N-linked glycosylation) and various protein kinase inhibitors (inhibitors of phosphorylation).

Specific aims

1) Identify whether glycosylation influence legumain processing and activation
2) Study whether glycosylation affects cellular transport of legumain.
3) Study whether glycosylation is important for legumain secretion.
4) Identify whether phosphorylation influence legumain processing and activation
5) Study whether phosphorylation affects cellular transport of legumain.

3 Materials and methods

3.1 Cell lines

3.1.1 Used cell lines

Two human colorectal cell lines were used in this study, SW620 and HCT116 (ATCC). HCT116 and SW620 cells are both adherent in culture, but have a distinct cellular morphology.

3.1.2 Cell storage

Cells were frozen and stored over longer periods of time in liquid nitrogen (-196°C), and thawed before use. For storage up to 6 months, the cells were frozen and stored at -70°C. To limit cell bursting and damage, a freezing solution (Appendix 1.1) containing 10 % of the cryoprotective agent dimethyl sulfoxide (DMSO) (Sigma-Aldrich) was added to the cells before freezing.

3.1.3 Thawing and cell culturing

Frozen cell ampoules with HCT116 and SW620 were thawed and then cultivated in T-75 flasks (Sigma-Aldrich) with 10 ml pre-warmed culture medium (Appendix 1.2) with or without 10 % foetal bovine serum (FBS) (PAA). The cells were grown in a humid environment at 37°C with 5 % CO_2, and all work with the cells was performed under sterile conditions in a LAF (Laminar Air Flow) bench. To remove residues of toxic DMSO (1 %), the medium was always replaced with fresh growth medium (Appendix 1.2) 16- 24 hours after thawing.

3.1.4 Passing and counting of cells

For passing or when seeding cells for experiments, the cells were detached from the growth surface using 1 ml trypsin/EDTA (Sigma-Aldrich) and diluted in fresh growth medium with serum according to cell density. Media containing serum was used to deactivate trypsin/EDTA. One fraction (1 ml) of cell solution was retained in the culturing flask (new

flask every third time) and fresh growth medium was added to a total of 10 ml for continued culturing. The other fraction was transferred to clean tubes and used for seeding or discarded. The cells were passed routinely twice a week to ensure that the cells did not grow too dense.

The cells were counted automatically before seeding for experiments. Briefly, 10 µl cell suspensions were mixed with 10 µl tryphan blue (Life technologies). Furthermore, 10 µl of the cell solution were applied into a chamber slide and counted using Countess Automatic Cell Counter (Invitrogen). The instrument calculates the total number of cells, including the number of live cells and the number of dead cells/ml cell suspension. The number of live cells/ml cell suspension was used to adapt the cell concentration and total number of cells required for the individual experiments.

3.2 Treatment of cells with inhibitors

3.2.1 Seeding of cells

HCT116 and SW620 cells were seeded (1.5 x 10^5/ml or 2.0 x 10^5/ml) in 6-well plates (Thermo Scientific) and left overnight for adherence to the plastic surface. The following day, the cellular morphology was observed in the microscope (Olympus) and the treatments were added directly into the wells. Control cells were always included. A brief description of used treatments in the present study follows.

3.2.2 Treatment with tunicamycin

Tunicamycin (Calbiochem) stock solution (10 mg/ml) was diluted 1:10 in DMSO, and added to the cells to obtain the following final concentrations: 1 µg/ml or 5 µg/ml. The control cells were added 10 µl DMSO. To obtain condition cell medium for immunoblotting, the medium was replaced with serum-free growth medium the day after seeding with the presences of tunicamycin. After incubation for 6, 24 or 48 hours, cells and serum-free conditioned medium were harvested (see section 3.3).

3.2.3 Treatment with staurosporine

Staurosporine (Calbiochem) stock solution (1mM) was diluted 1:10 in DMSO, and added to the cells to obtain the following final concentrations: 0.2, 0.6 or 1 µM. The control cells were

added 10 µl DMSO. The cells were incubated for 0.5 or 6 hours before harvesting (see section 3.3).

3.2.4 Treatment with H7

H7, dihydrochoride (Calbiochem) stock solution (50 mM) was diluted 1:10 in double distilled water (ddH_20), and added to the cells to obtain the following final concentrations: 5, 15, or 30 µM. The control cells were added 10 µl ddH_20. The cells were incubated for 1 hour before harvesting (see section 3.3).

3.3 Harvesting of cells and conditioned media

Harvesting of cells and serum-free conditioned media were performed to obtain samples for immunoblotting.

Conditioned media (with serum) were removed, and the adherent cells were carefully washed 3 times in cold 1 X Phosphate-buffered Saline (PBS) (Lonza). Subsequently, the cells were lysed with 75 µl cold lysis buffer (Appendix 2.2) and scraped off by the use of a rubber policeman (TPP). The cell lysates were transferred to Eppendorf tubes (Thermo Scientific) and centrifuged at 13000 x g for 15 minutes at 4°C. Further, the supernatants were transferred to clean tubes on ice. To prevent degradation, the samples were kept on ice and cold temperature at all times after cell lysis.

Serum-free conditioned media were collected and centrifuged at 500 x g for 5 minutes. Subsequently, the supernatant were transferred to Eppendorf tubes on ice. Proteins in the conditioned medium were concentrated by addition of 4 volumes of ice cold acetone (Merck), leaving the sample on ice for 15 min and centrifugation at 4°C and 12000 x g for 10 min. Liquid was removed and the precipitate air dried at room temperature before re-dissolving in 40 µl lysis buffer (Appendix 2.2). Cell lysates and conditioned media were stored at -70°C for downstream analysis.

3.4 PNGase F and Endo H treatment

Cell lysates treated with tunicamycin or DMSO (control) as described in 3.2.2, were further treated by using PNGase F or Endo H kit (New England BioLabs). The experiments were

performed according to the manufactures protocol. In brief, 20- 40 µg samples were mixed with 10 X glycoprotein denaturing buffer (1/10 of total calculated volume) and the reaction mix was denatured at 100°C for 10 minutes. The tubes with denatured solution was either added 1µl (=500 units) PNGase F, or 1µl (=500 units) Endo H. To the control lysates, 1 µl ddh20 were added instead of the enzymes. The reaction mix was finally incubated at 37°C for 1 hour at gentle mixing before the samples were stored at -70 °C for further analysis.

3.5 Subcellular enrichment

Isolation and enrichment of proteins in the cellular fractions cytosol, membrane/lysosomes, nucleus and cytoskeletal were performed using the Subcellular Protein Fractionation Kit for Cultured Cells (Thermo Scientific). The protocol was followed as recommended by the manufacture, additionally washing of the pellet between the first two fractions were performed to reduce contamination and to ensure high purity.

3.5.1 Cell culture preparation

HCT116 cells were seeded in T-250 flasks (Sigma-Aldrich) one day prior to treatment with tunicamycin (5 µg/ml) and DMSO (10 µl). After 24 hours incubation, the cells were detached using trypsin/EDTA and suspended in 1 ml cold 1 X PBS. The cell suspension was transferred to a 15 ml tube and pelleted by centrifugation at 500 x g for 5 minutes. Subsequently, the pellet was resuspended in cold PBS and pelleted by centrifugation at 500 x g for 5 minutes. The supernatant were removed, and the last step was repeated (at 4°C).

3.5.2 Subcellular enrichment

The fractionation kit contained extraction buffers, proteinase inhibitors, micrococcal nuclease and calcium chloride ($CaCl_{2)}$. An overview of the buffers and volume used in this protocol is depicted in Table 3.1. The buffers were thawed and added proteinase inhibitor immediately before use. Cytoplasmic extraction buffer (CEB), Membrane extraction buffer (MEB) and nuclear extraction buffer (NEB) were kept on ice at all times.

Table 3.1: Buffer types and volume utilized in subcellular enrichment.

	Cytoplasmic extraction buffer (CEB)	Membrane extraction buffer (MEB)	Nuclear extraction buffer (NEB)	Pellet extraction buffer (PEB)
Used to isolate proteins from	Cytosol	Lipid membranes and intramembranous content	Nucleus	Cytoskeletal
Volume buffer (µl)	300	300	100	100
Proteinase inhibitor (1:100) (µl)	3	3	1	1

The cell pellet obtain in section 3.5.1 was resuspended in cold CEB and incubated at 4°C for 10 minutes on a rotary shaker. Further, the cell suspension was centrifuged at 500 x g for 5 minutes, and the supernatant (cytoplasmic fraction) was transferred to a clean tube on ice. The pellet was washed by adding CEB, centrifugation at 500 x g for 5 minutes before the supernatant was removed. Subsequently, the pellet was resuspended in cold MEB, vortexed at a high speed and incubated at 4°C for 10 minutes. The suspension containing MEB was centrifuged at 3000 x g for 5 minutes, and the supernatant (membrane fraction) was transferred to a clean tube on ice. After washing the pellet with MEB, ice cold NEB was added to the pellet and then mixed by vortexing. Further, the suspension was incubated at 4°C for 30 minutes on a rotary shaker, centrifuged at 5000 x g for 5 minutes before the supernatant (soluble nuclear extract) were transferred to a clean tube on ice. Subsequently, room temperature NEB (containing 5 µl $CaCl_2$ and 3 µl micrococcal nuclease) was added to the pellet and then mixed by vortexing. The suspension was incubated at 15 minutes at room temperature, vortexed at a high for 15 seconds and centrifuged 16000 x g for 5 minutes. The supernatant (chromatin-bounded nuclear fraction) was transferred to a clean tube on ice. Finally, to obtain the cytoskeletal extract, room temperature PEB were mixed with the pellet by vortexing, incubated at room temperature for 10 minutes and centrifuged at 16000 x g for 5 minutes. All the fractions were stored at -70°C for further analysis.

3.6 Total protein concentration measurements

The protein concentration of each cell lysates was measured using bicinchoninic acid (BCA) protein assay kit (Pierce). This is a colorimetric method based on the biuretic reaction (proteins reduce the copper ions from Cu^{2+} to Cu^{1+} in an alkaline environment) where Cu^{1+}

forms a purple colored complex with a reagent containing bicinchoninic acid (BCA). The BCA/copper complex exhibits strong absorbance at 562 nm and the amount of reduced Cu^{2+} is proportional to the amount of total protein present in the samples.

Duplicates (25 µl) of albumin standards (BSA), samples, and negative control (ddH_20) were added to a 96-well plate (Thermo Scientific). The samples were diluted 1:5 in ddH_20, and the BSA standard was diluted in ddH_20 at the following concentrations (µg/ml): 1500, 1000, 750, 500, 250 and 125. The BCA working reagent was prepared by mixing BCA reagent A with BCA reagent B (50:1, Reagent A: B) and 200 µl were added to each well. Further, the plate was incubated for 30 min at 37°C, and the absorbance was measured at 540 nm for 1 second on the plate reader (Modulus microplate). The total protein concentration in the cell lysates was calculated from a standard curve based on the absorbance of the albumin standards.

3.7 Immunoblotting (Western blotting)

Immunoblotting is used in research to detect specific proteins using antibodies after separation by gel electrophoresis.

According to the total protein concentrations measurements described in chapter 3.6, the cell lysates were diluted in ddH_20 to obtain chosen amounts of total protein in each loaded sample. Subsequently, each diluted samples were mixed with lithium dodecyl sulfate (LDS, replacing SDS) (Invitrogen) and a reducing agent containing dihiothreitol (DTT) (Invitrogen) before boiling at 95°C for 5 min. LDS and heating unfolds the protein of interest (i.e. denaturation) and gives the proteins a uniform negative charge. DTT helps to further denaturation by breaking disulfide bonds that contributes to the three-dimensional structure of proteins. Samples, SeeBlue protein standard (Invitrogen) and recombinant human prolegumain (rhLeg) (R&D systems) were subsequently loaded on a gradient polyacrylamide gel (4-12 % NuPAGE gel, Invitrogen), placed in a gel electrophoresis chamber with MES buffer (Appendix 3.1). The electrophoresis was run on 150 V for 1 hour and 15 min. The proteins migrate during electrophoresis towards the positive electrode and separate according to size. Smaller proteins migrate faster than larger proteins which are delayed in a porous matrix such as polyacrylamide gel.

After separation the proteins were blotted onto a polyvinylidene difluoride (PVDF) (Life Technologies) membrane. The membrane is highly hydrophobic and must be activated in

methanol (VWR) before soaking in transfer buffer (Appendix 3.2). Whatman paper and sponge pads for blotting were also soaked in transfer buffer. The blotting equipment was layered in the following order: 3 sponge pads / Whatman paper / gel / membrane / Whatman paper / 3 sponge pads. Air bubbles were removed by rolling a pipette over the stack, and the equipment was installed into a transfer tank containing transfer buffer. The blotting was done at constant current (400 mA) for 1 hour at 4°C.

To prevent nonspecific bonding of antibodies to the membrane, it was blocked with 5 % dry fat-free milk (Tine meierier) TBST-buffer (Tris-Buffered Saline with Tween 20) (Appendix 3.3) for 1 hour at room temperature with gentle shaking. Subsequently, the membrane was incubated with primary antibody for 1 hour and washed 3 times for 10 minutes in TBST buffer. Then, the membrane was incubated with secondary antibody for 1 hour and washed 3 times for 10 minutes in TBST-buffer. The primary antibodies specifically target the proteins of interest, and the secondary specifically targets the primary antibody. The antibodies were diluted in 5 % dry fat-free milk TBST-buffer, and the used antibodies can be seen in Table 3.2.

The secondary antibodies are conjugated with the enzyme horseradish peroxidase (HRP), and a chemiluminescent light complex was formed by the addition of SuperSignal West Dura Extended Duration Substrate (Pierce). The light was detected by a light sensitive camera (G:BOX- Syngene). Image analysis was carried out using GeneSnap and GeneTools. The standard, which contains colored proteins of known sizes, was used to estimate the size and to identify the proteins on the immunoblots.

Table 3.2: Antibodies utilized in immunoblotting.

Protein	Primary antibody	Dilution	Secondary antibody	Dilution
Legumain	Goat anti-human legumain polyclonal antibody (R&D Systems)	1:1000	Rabbit Anti-Goat immunoglobulins/HRP (Dako)	1:5000
α –Tubulin	Mouse anti-α –tubulin monoclonal antibody (Calbiochem)	1:5000	Rabbit Anti-Mouse immunoglobulins/HRP (Dako)	1:5000
Arylsulfatase B (ARSB)	Mouse anti-ARSB monoclonal antibody (R&D Systems)	1:500	Rabbit Anti-Mouse immunoglobulins/HRP (Dako)	1:5000
Specificity protein 1 (SP1)	Rabbit anti-SP1 polyclonal antibody (Millipore)	1:10000	Goat Anti-Rabbit immunoglobulins/HRP (Dako)	1:5000

3.7.1 Cell viability measurement (MTS)

The cell viability was measured using the CellTiter 96 AQ_{ueous} One Solution Cell Proliferation Assay (also called MTS assay) (Promega) according to the manufactures protocol. The assay contains the tetrazolium compound MTS (3-4,5-dimethylthiazol-2-yl)-5-(3-carboxymethoxyphenyl)-2-(4-sulfophenyl) and the electron coupling reagent PES (phenazine etosulfat). In brief, the MTS compound is reduced by viable cells into to a formazan product. The reduction is presumed to be caused by NADPH or NADH produced by dehydrogenase enzymes in metabolically active cells. Formazan is a brown colored product, and the quantity produced is directly proportional to the number of living cells.

HCT116 cells were seeded in triplicates in a 96-well plates (Thermo Scientific) with the same number of cells in each well (1.4 x 10^4 cells in a volume of 100 µl), and were incubated overnight. The next day, tunicamycin or DMSO was added directly to the cell medium. At the day of measurement, 20 µl MTS was added to each well. The cells were incubated for 1 hour, and the absorbance was measured 490 nm for 1 second on the plate reader (Modulus microplate).

3.8 Indirect immunofluorescence

Immunofluorescence is a biochemical labeling technique for detection of specific proteins. There are two main methods of immunofluorescence labeling, direct and indirect

immunofluorescence. The indirect immunofluorescence method, where the secondary antibody is labeled with a fluorochrome, was used in this study to detect legumain, endosomes and lysosomes in HCT116 cells. The nucleus was stained with the fluorochrome 4',6-diamidino-2-phenylindole (DAPI). DAPI intercalates with A-T rich regions of DNA and forms a fluorescent complex, and do not require use of a secondary antibody for detection. The cells were detected by using a fluorescence microscope (Olympus) and a confocal microscope (Carl Zeiss LSM710).

HCT116 cells were cultured on sterilized glass slides (Thermo scientific) (2.0 x 10^5/ml) in a 6-well plate and incubated at 37°C, 5 % $C0_2$. To ensure high cell attachment to the glass slides, the cells were incubated for two days before treatment with tunicamycin. After 24 hours, the lysosomes were labeled in live cells using 75 nM Lysotracker Red DND-99 (Life technologies) for 1 hour at 37°C. Lysotracker is a permeable fluorescent dye which label acidic organelles in live cells.

The cultured cells were washed 3 times for 5 minutes with cold PBS, fixed for 15 minutes with 4 % cold paraformaldehyde (PFA) (Chemi-teknik) (Appendix 4.2), and then washed 3 times for 5 minutes with 200 mM Hepes (Appendix 4.1) and 3 times for 5 minutes with 1X PBS. Subsequently, the cells were permeabilized with 0.2 % Triton-X100 (VWR) (Appendix 4.5) for 5 minutes and washed 4 times for 5 minutes with 1X PBS, and blocked with 3 % horse serum (HS) (Sigma-Aldrich) (Appendix 4.3) at 37°C for 1 hour. After two subsequent wash for 5 minutes with 1X PBS and 0.1 % HS (Appendix 4.4), the coverslips were transferred to a moisturized incubation chamber. Furthermore, 50 µl primary antibody (Table 3.3) diluted in 0.1 % HS were added to each coverslips and incubated overnight at 4°C. The following day, the coverslips were transferred back to the 6-well plate and washed 6 times for 5 minutes with 0.1 % HS. Subsequently, the coverslips were incubated in the moisturized incubation camber with diluted secondary antibody (Table 3.3) in 0.1 % HS for 60 minutes at 37°C, and washed 3 times for 5 minutes with 0.1 % HS. The staining process was repeated (using different antibodies, Table 3.3) and the cells were washed 3 times for 5 minutes with 1X PBS and 1 minute with ddH_20. ProLong Gold antifade reagent with DAPI (Life technologies) was applied on microscope slides before mounting the coverslips. The slides were finally harden for 1 hour at room temperature, and stored at 4°C for further analysis.

Table 3.3: Antibodies utilized in immunofluorescences.

Protein	Primary antibody	Dilution	Secondary antibody	Dilution
Early endosomes antigen 1 (EEA1)	Rabbit EE1-antibody (Santa Cruz)	1:100	Alexa Fluor® 488 donkey anti-rabbit antibody (Jackson ImmunoResearch)	1:300
Legumain	Goat anti-human legumain polyclonal antibody (R&D systems)	1:100	Alexa Fluor® 594 donkey anti-goat antibody (Jackson ImmunoResearch)	1:300

4 Results

4.1 Legumain and N-linked glycosylation

4.1.1 Determination of tunicamycin concentrations and incubation time

To investigate the effect of tunicamycin on HCT116 and SW620 cells, the cells were treated with various concentrations of tunicamycin for 6 or 48 hours. The cell morphology and legumain expression were analyzed by light microscopy and immunoblotting, respectively.

Normal cellular morphology was maintained following treatment (not shown). The control cells, as well as the tunicamycin-treated cells, were elongated and attached to the well surface.

Immunoblotting demonstrated that HCT116 and SW620 control cells displayed glycosylated prolegumain (56 kDa) and mature legumain (36 kDa), although to a different extent (Fig. 4.1 A). HCT116 cells expressed mainly mature legumain, while SW620 predominantly expressed the proform. In tunicamycin-treated cells, the proform of 56 kDa was converted to a band at 47 kDa. Demonstrating a noticeable mass shift corresponding to previous studies (Fig. 1.7, Haugen *et al.*, unpublished data), indicate the presence of prolegumain without glycan groups attached. Moreover, tunicamycin seemed to inhibit glycosylation in a dose- and time-dependent manner. Increased levels of unglycosylated prolegumain (47 kDa) were observed in cells treated with 5 µg/ml tunicamycin for 24 hours, whereas unglycosylated legumain was absent or expressed at a very low level when cells were treated under other incubation conditions (time/dose) (Fig. 4.1).

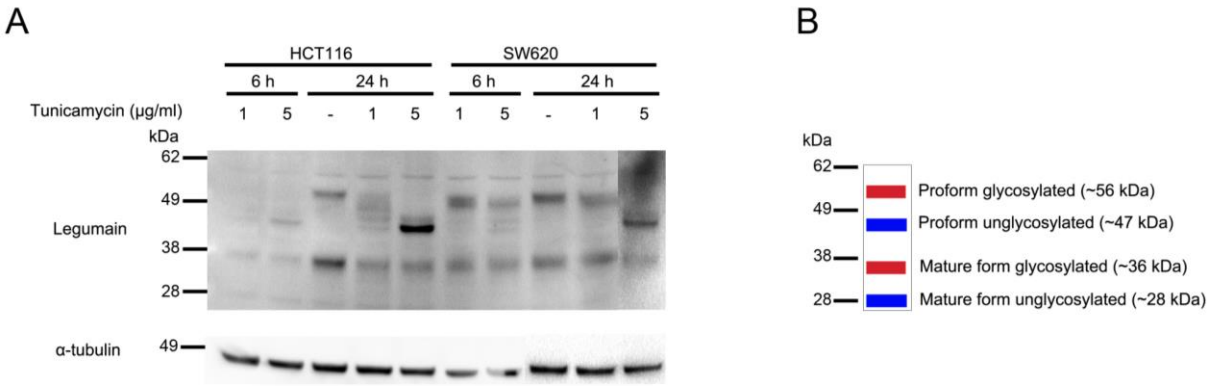

Figure 4.1: Legumain expression in HCT116 and SW620 cells treated with tunicamycin. (A) The cells were treated with tunicamycin using the indicated concentrations and exposure times. The control cells were treated with 10 µl DMSO. Protein expression was analyzed by electrophoresis and immunoblotting. All lanes were loaded with 25 µg total protein. The filters were stained with a specific antibody against legumain (upper panel) and α-tubulin (loading control, lower panel) (n=1). (B) Estimated protein band size of the glycosylated and unglycosylated forms of legumain.

Based on these initial experiments, it was chosen to use a tunicamycin concentration of 5 µg/ml and exposure length of 24 hours in the following experiments. In addition, we decided to focus on the HCT116 cell line.

4.1.2 Effect of tunicamycin on cell viability

MTS assay was used to measure cell viability in HCT116 cells after treatment with 0, 2.5 or 5 µg/ml tunicamycin for 24 hours. The viability of the treated cells relative to control is shown in Figure 4.2. Major differences in cell viability between control and tunicamycin-treated cells were not observed.

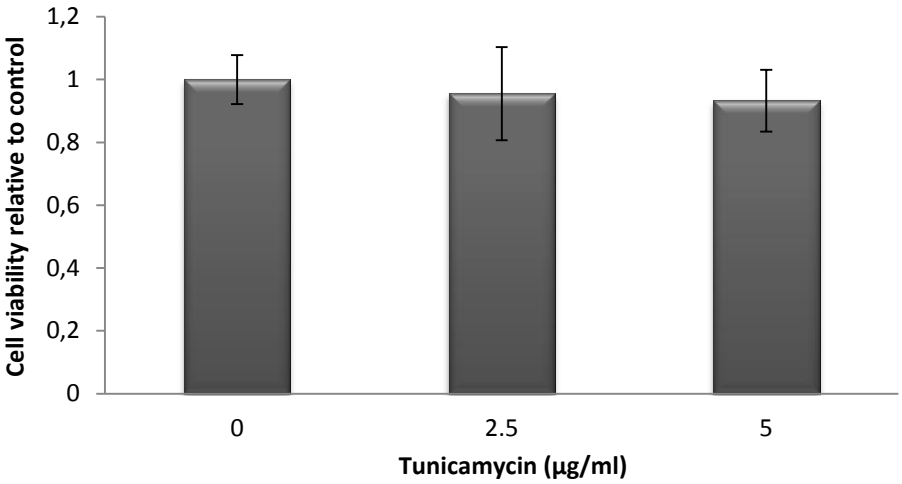

Figure 4.2: Cell viability of HCT116 cells treated with tunicamycin. HCT116 cells were treated with 2.5 or 5 µg/ml tunicamycin and presented relative to control. The control cell was treated with 5 µl DMSO. The figure shows the mean values ± SEM (n=3).

4.1.3 Determination of N-linked glycosylation groups on the legumain protein

It has been identified that mammalian legumain has at least three distinct occupied glycosylation seats (Haugen *et al.*, unpublished data, as shown in chapter 1.8.3). Therefore, it was of interest to study whether the observed 47 kDa form in tunicamycin-treated cells represents fully unglycosylated legumain. The cell lysates were treated with PNGase F, an enzyme which removes N-linked glycosylation. Furthermore, it was of interest to determine the type of N-linked glycosylation. To investigate this, cell lysates were treated with Endo H, which only cleaves the high mannose and hybrid type oligosaccharides.

HCT116 cells were treated with or without 5 µg/ml tunicamycin for 24 hours, based on the results from the initial experiments. The cell lysates were further treated with 1 µl (=500 units) PNGase or Endo H. Control lysates were added 1 µl ddH_20. Legumain expression and processing were analyzed by immunoblotting.

Immunoblotting of cell lysates treated with PNGase F is shown in Figure 4.3 A. HCT116 control lysates expressed 56 kDa prolegumain and 36 kDa mature legumain, though the latter to a higher extent (Fig. 4.3 A). In cells treated with tunicamycin alone, 56 kDa prolegumain was converted to 47 kDa prolegumain. Some mature glycosylated legumain of 36 kDa could also be observed. PNGase F treatment as well as the combination of tunicamycin and PNGase

F resulted in a shift in the apparent molecular mass from 56 kDa to approximately 47 kDa for the proform and from 36 kDa to 28 kDa for the mature form of legumain (Fig. 4.3 A), although less of the 28 kDa glycosylated mature form was observed in double treated cells. The immunoblot demonstrated an identical shift of the molecular mass of glycosylated legumain after treatment with PNGase F and the combination with tunicamycin. This indicates that legumain is fully unglycosylated upon treatment with 5 µg/ml tunicamycin for 24 hours.

Immunoblotting of cell lysates treated with Endo H is shown in Figure 4.3 B. HCT116 control lysates expressed 56 kDa prolegumain and 36 kDa mature legumain, though the latter to a higher extent (Fig. 4.3 B). In cells treated with tunicamycin alone, 56 kDa prolegumain was converted to 47 kDa prolegumain. Some mature glycosylated legumain of 36 kDa could also be observed. Endo H treatment as well as the combination of tunicamycin and Endo H resulted in a shift in the apparent molecular mass to approximately 47 kDa prolegumain and 28 kDa mature legumain (Fig. 4.3 B), although less of the 28 kDa glycosylated mature form was observed in the double treated cells. Taken together, tunicamycin treatment alone, Endo H treatment and the combination, gave identical shifts of the molecular mass of glycosylated legumain. The similar shift in molecular mass of legumain from cells treated with PNGase F and Endo H indicates that all attached N-glycans are of the high mannose or hybrid types.

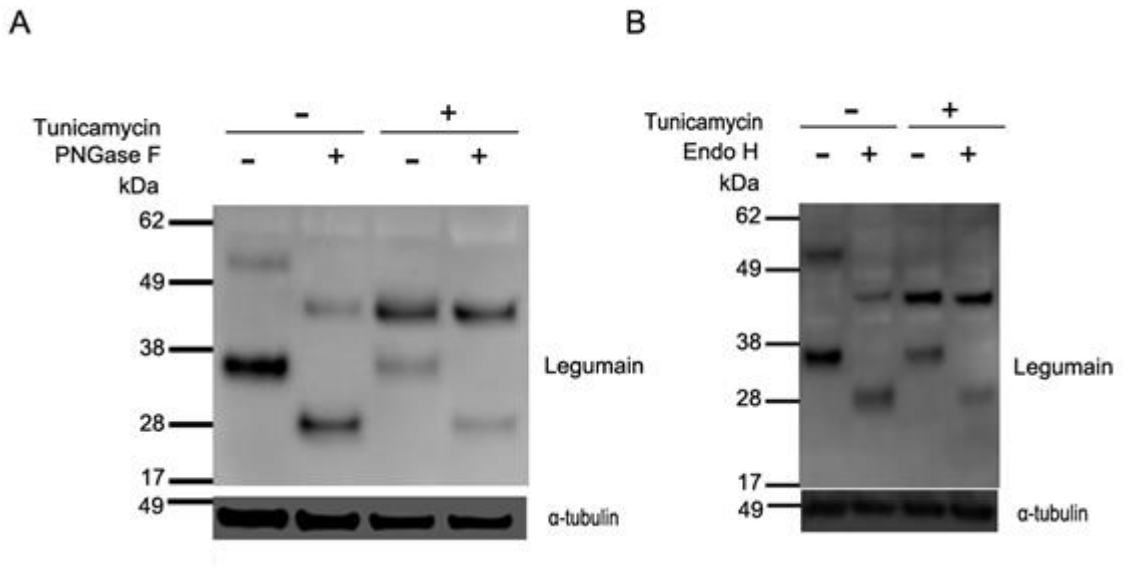

Figure 4.3: Immunoblot of legumain expression in HCT116 cells when deglycosylated by treatment with PNGase F (A) or Endo H (B). HCT116 cells were treated with or without 5 µg/ml tunicamycin. The control cells were treated with 10 µl DMSO. After 24 hours the cells were harvested and treated with 500 units PNGase F (A) or Endo H (B). Control lysates were added 1µl ddh20. Protein expression was analyzed with electrophoresis and immunoblotting. The lanes were loaded with 30 µg (A) or 15 µg (B) total protein. The filters were stained with a specific antibody against legumain (upper panel) and α-tubulin (loading control, lower panel) (n=1).

4.1.4 Increased presence of prolegumain in tunicamycin-treated HCT116 cells

The initial experiments demonstrated that processing to non-glycosylated mature legumain (28 kDa) were totally absent after tunicamycin treatment for 24 hours. It was therefore of interest to examine whether 28 kDa legumain would appear after tunicamycin treatment for a prolonged period. We also hypothesized that the presence of glycosylated 36 kDa mature legumain was due to the maturation of glycosylated prolegumain synthesized prior to treatment. In order to investigate this, HCT116 cells were treated with 5 µg/ml tunicamycin for 48 hours. Cell morphology and legumain expression were analyzed by light microscopy and immunoblotting, respectively.

Light microscopy demonstrated that the cellular morphology changed slightly after treatment with tunicamycin for 48 hours. The control cells were elongated, while the treated cells

seemed smaller with an irregular form. In addition, there were observed multiple detached cells following treatment (not shown).

Legumain processing to the 28 kDa unglycosylated mature form were still not observed after treatment for 48 hours with tunicamycin, resulting in an accumulation of the unglycosylated proform (47 kDa). Although, small amounts of the glycosylated mature form (36 kDa) were still detected in the cell lysates (Fig. 4.4).

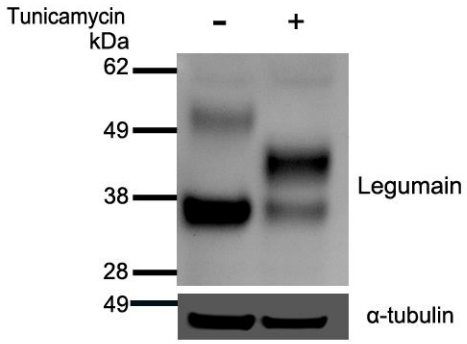

Figure 4.4: Legumain expression in HCT116 cells treated with tunicamycin for 48 hours. The cells were treated with or without 5 µg/ml tunicamycin. The control cells were treated with 10 µl DMSO. After 48 hours the cells were harvested and the protein expression was analyzed by electrophoresis and immunoblotting. Both lanes were loaded with 30 µg total protein. The filters were stained with a specific antibody against legumain (upper panel) and α-tubulin (loading control, lower panel) (n=1).

4.1.5 Tunicamycin treatment resulted in altered localization of legumain in HCT116 cells

Having observed cellular accumulation of non-glycosylated prolegumain, it was of interest to visualize the distribution of glycosylated versus unglycosylated legumain by immunofluorescence confocal microscopy. HCT116 cells were cultured on glass slides, treated with or without 5 µg/ml tunicamycin and fixed with PFA. After fixation, the cells were stained for legumain and the nucleus. The nucleus was labeled using DAPI, which adheres to the double stranded DNA and emits light at 461 nm (blue light). The pseudo-coloring of the images was performed using software (ZEN 2012).

Representative confocal pictures of untreated (A) and tunicamycin-treated (B) cells are depicted in Figure 4.5. The cell nucleus seemed to be round and intact in both control and treated cells (left, top panels). Moreover, the cell shape was also intact and did not show any

signs of deformation after treatment (left, lower panels). Thus, the cellular morphology was apparently not affected by the tunicamycin treatment. Legumain appeared to be vesicular distributed in both untreated and treated cells. Interestingly, there were clear differences between legumain expression in treated and untreated cells. Legumain gave rise to more intense signal in the treated cells than the untreated, and seemed to be accumulating after tunicamycin treatment.

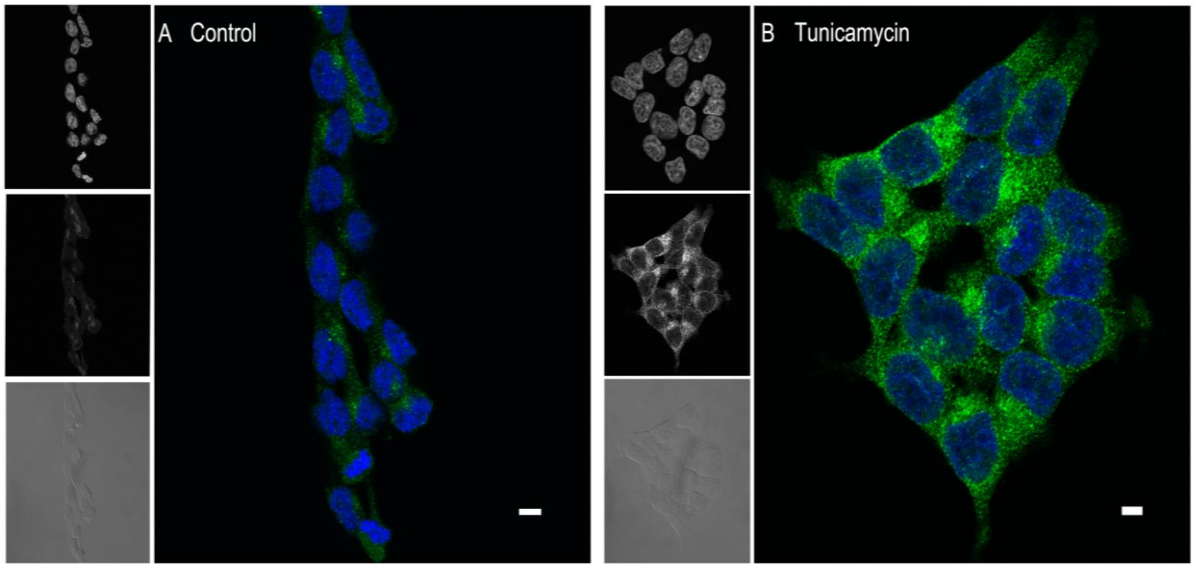

Figure 4.5: **Confocal images of legumain in HCT116 cells.** The cells were culture on sterile glass slides and treated with 10 µl DMSO (A) or 5 µg/ml tunicamycin (B) for 24 hours. After fixation the cells were stained with a specific antibody against legumain and with DAPI. The cells were visualized using confocal microscopy with 63X objective. The merged picture of legumain (green) and the nucleus (blue) are shown to the right. The nucleus (white, upper left panels), legumain (white, middle left panels) and phase contrast picture of the cell (grey, lower left panels) are shown to the left. Scale bars represent 5 µm. One representative of n=4 experiments is shown.

4.1.6 Expression of unglycosylated legumain in subcellular fractions and in conditioned medium

Legumain is thought to be targeted to and activated in the lysosomes. So far, it is not known whether glycosylation is required for transport to the lysosomes. To investigate intracellular distribution of unglycosylated legumain, we enriched proteins from various intracellular compartments of HCT116 cells treated with or without 5 µg/ml tunicamycin for 24 hours. Furthermore, it was also of interest to examine whether secretion was independent of glycosylation. To study this, serum free conditioned media derived from HCT116 cells was

collected 24 hours after treatment with or without 5 µg/ml tunicamycin. Cell lysates from each enriched fraction, total cell lysates and corresponding conditioned growth medium were analyzed by immunoblotting for the presence of glycosylated and unglycosylated legumain (Fig. 4.6).

In the cytosolic fraction, small amounts of unglycosylated prolegumain (47 kDa) and glycosylated mature legumain (36 kDa) were observed in tunicamycin-treated cell lysates, whereas only 36 kDa mature legumain were detected in control lysates. Moreover, HCT116 control cells displayed low levels of glycosylated proform and high levels of glycosylated mature form in the membrane/endo-lysosomal fraction. By comparison, in tunicamycin-treated cells, substantial amounts of unglycosylated prolegumain (47 kDa) and low levels of glycosylated mature legumain (36 kDa) were detected in the membrane/endo-lysosomal fraction. In the nucleus fraction, substantial amounts of glycosylated prolegumain and low levels of glycosylated active legumain were observed in the control lysates. Interestingly, in tunicamycin-treated cell lysates, unglycosylated prolegumain and glycosylated mature legumain were expressed at a very low level in the nuclear fraction, which indicate that glycosylation is important for legumain transport into the cell nucleus (Fig. 4.6, upper panel).

Compartment specific protein markers (with presumed limited distribution) were used as purity controls. Arylsulfatase B (ARSB) and specificity protein 1 (SP1) were used for the membrane/endo-lysosomal and nucleus fractions, respectively. Substantial levels of ARSB were found in the membrane/endo-lysosomal fractions, while almost no detectable amounts were found in the other fractions (Fig. 4.6, middle panel). The highest level of SP1 was detected in the nucleus fractions, and only low levels were detected in the other fractions (Fig. 4.6, lower panel). The protein markers demonstrated that there was good enrichment of each subcellular compartment.

Glycosylated prolegumain of 56 kDa was found to be secreted and detected in the conditioned media derived from untreated HCT116 cells. Of particular interest was the equal presence of non-glycosylated prolegumain (47 kDa) in the conditioned media derived from tunicamycin-treated cells. Moreover, the mature form was undetectable in conditioned media from both treated and untreated cells (Fig. 4.6, upper panel).

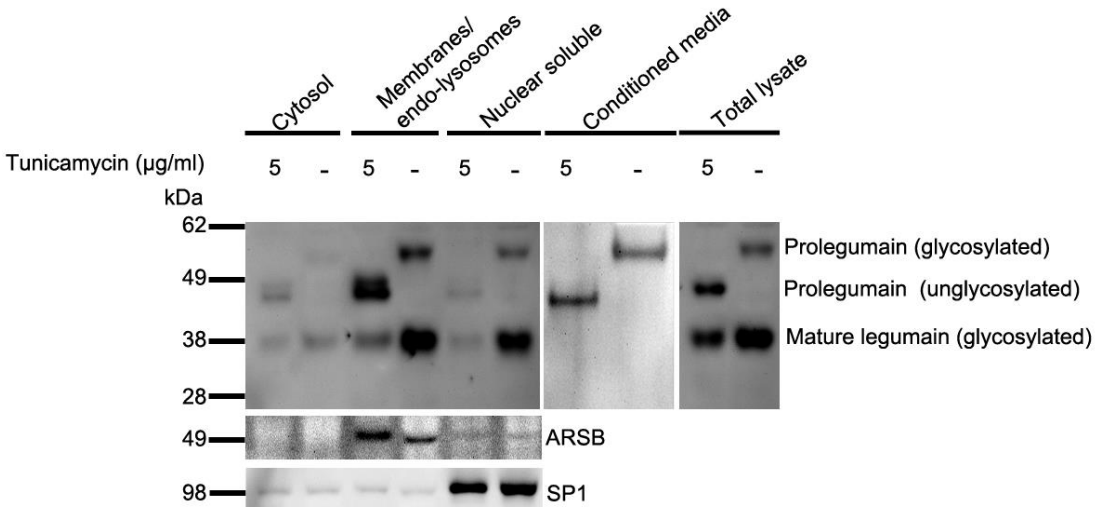

Figure 4.6: Subcellular localization of legumain from HCT116 cells treated with tunicamycin. The cells were treated with 5 µg/ml tunicamycin for 24 hours. The control cells were treated with 10 µl DMSO. Protein expression was analyzed by electrophoresis and immunoblotting. The lanes were loaded with 7 µg total protein form each intracellular fraction (upper, left panel) or 30 µg total protein from the total cell lysates (upper, right panel). Conditioned media was concentrated by acetone- precipitation, and similar volumes were added to the lanes (upper, middle panel). The filters were stained with a specific antibody against legumain (upper panels). Purity control of the subcellular fractions were assessed by staining for ARSB (soluble lysosomal protein) and SP1 (nuclear transcription factor), depicted in middle and lower panels (n=1).

4.1.7 Endo-lysosomal distribution of unglycosylated legumain?

Immunofluorescence confocal microscopy was used to visualize whether non-glycosylated legumain was transported to the endosomes and lysosomes. Control and tunicamycin-treated HCT116 cells were stained for legumain, endosomes, lysosomes and the nucleus. Lysosomes were labeled in live cells using Lysotracker, while legumain and the endosomes were stained after fixation using a specific antibody against legumain and early endosomes antigen 1 (EEA1), respectively. The nucleus was labeled using DAPI, and the pseudo-coloring of the images was performed using software (ZEN 2012).

Figure 4.7 represents untreated (A) and tunicamycin-treated (B) cells stained for legumain and early endosomes antigen 1 (EEA1). The merged pictures of legumain (red) and EEA1 (green) are shown in the right panels and some overlap of green and red are seen as yellow spots after tunicamycin treatment (B), which may represent colocalization of legumain and EEA1. In contrast, overlap of EEA1 (green) and legumain (red), i.e. yellow spots, in the control cells were not observed.

Confocal microscopy pictures of cells labeled with specific antibody against legumain and Lysotracker are depicted in Figure 4.7 C and D. The merged pictures of legumain (red) and Lysotracker (green) of untreated (C) and tunicamycin-treated (D) cells showed some overlap of red and green colors, i.e. yellow spots, indicating colocalization and thus of legumain in the lysosomes.

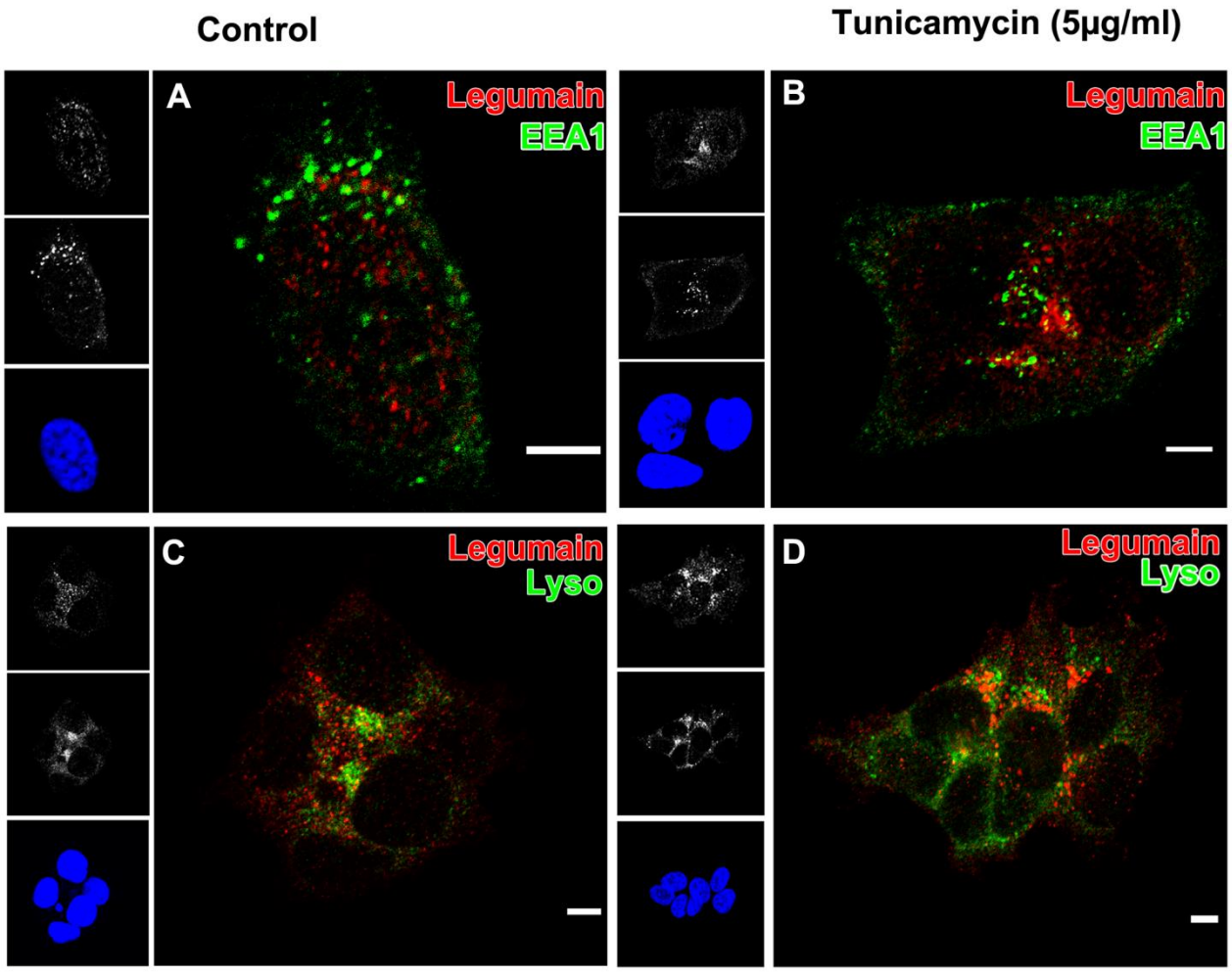

Figure 4.7: Endo-lysosomal localization of legumain in HCT116 cells treated with Tunicamycin. HCT116 cells were cultured on sterile glass slides and treated with 5 µg/ml tunicamycin (B and D) or 10 µl DMSO (A and C) for 24 hours. After fixation the cells were stained with specific antibodies and visualized using confocal microscopy with 63 X objective. (A and B) Cells stained for the nucleus (blue), legumain (red) and EEA1 (green). The left panels (from the top) represent legumain, EEA1 and the nucleus. (C and D) Cells stained for the nucleus (blue), legumain (red) and Lysotracker (Lyso; green). The left panels (from the top) represent legumain, Lysotracker and the nucleus. Scale bars represent 5 µm. One representative of n=3 experiments is shown.

4.2 Legumain and phosphorylation

4.2.1 Effect of protein kinase inhibitors on legumain processing and expression

To investigate the potential connection between legumain processing and phosphorylation, HCT116 and SW620 cells were treated with staurosporine, a broad spectrum protein kinase inhibitor. Initially the cells were treated with final concentrations of 0, 0.2, 0.6 or 1 µM staurosporine for 6 hours.

The cellular morphology was visualized using light microscopy. The observations are shown in Figure 4.8, where cells treated for 6 hours are shown in the upper panels. Morphological characteristics of both HCT116 and SW620 cells changed after staurosporine treatment for 6 hours. Cells treated with staurosporine had an irregular shape, with black and thin branches protruding from the cell body. In contrast, there were not observed branches in the control cells. Based on these observations, the treatment time was reduced to 0.5 hour (Fig. 4.8, lower panels). There were still observed differences in the cell morphology between control and staurosporine-treated (1 µM) cells for both cell lines. However, there were also observed differences in the cellular morphology of the HCT116 control cells. Control cells after 0.5 hour treatment were elongated (lower, left panel), whereas the control cells after 6 hours treatment were small and non-elongated (top, left panel).

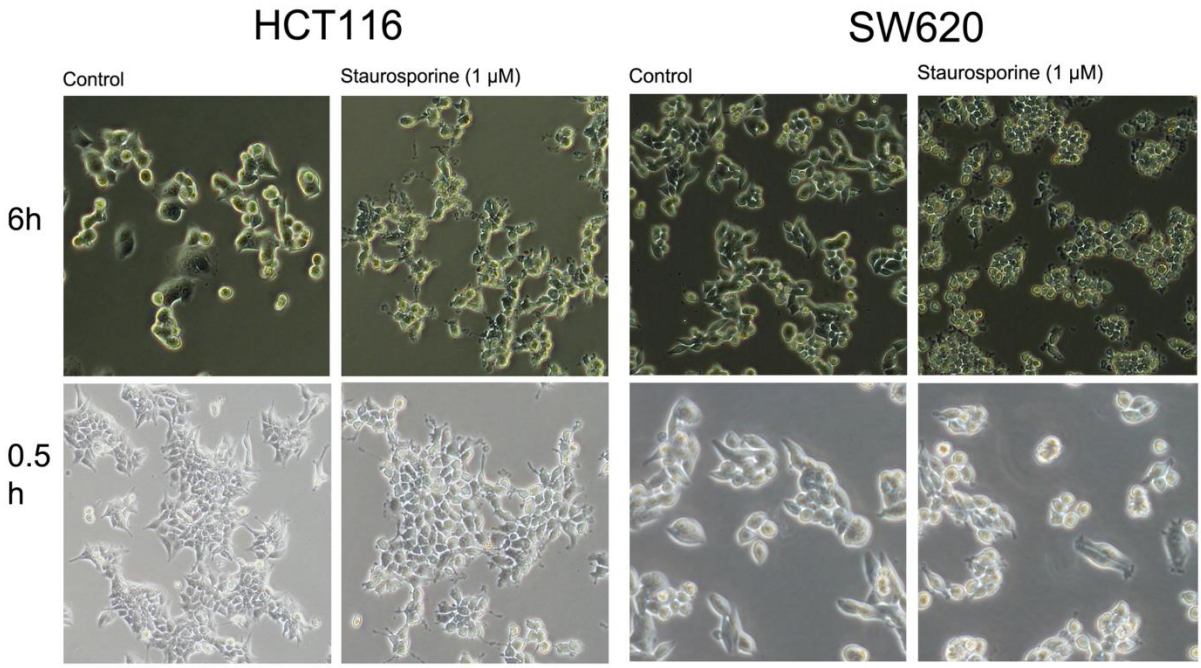

Figure 4.8: Effect of staurosporine on the cell morphology of HCT116 and SW620 cells. The cells were treated with 1 µM staurosporine for 6 (upper panels) or 0.5 hours (lower panels). The control cells were treated with 10 µl DMSO. Morphology of the cells were visualized using light microscopy with 10X (left panels, HCT116) or 20X (right panels, SW620) objectives.

Legumain expression and processing were analyzed by immunoblotting. Immunoblot of the cell lysates after staurosporine treatment for 0.5 hour is shown in Figure 4.9 A. In both control and staurosporine-treated cells, legumain appeared to be present as prolegumain (56 kDa) and mature legumain (36 kDa), although at different levels in HCT116 and SW620 cells as previously observed. HCT116 cells expressed mainly mature legumain, while SW620 expressed higher levels of the proform than the mature form. Similar results were seen after treatment for 6 hours (not shown). The immunoblots after staurosporine treatment for 6 and 0.5 hours gave the impression that there were apparently no alterations in legumain expression or processing with or without staurosporine treatment. Total intensities of legumain relative to α-tubulin (loading control) following staurosporine treatment are shown in Figure 4.9 B (HCT116) and C (SW620). The loading control α-tubulin was used to normalize the band intensities of legumain. There were some variations in the total expression of legumain between controls and treated cells. However, as the densitometric scanning showed that staurosporine gave rise to both increased and decreased total legumain expression, it was difficult to draw any conclusions (Fig. 4.9 B and C).

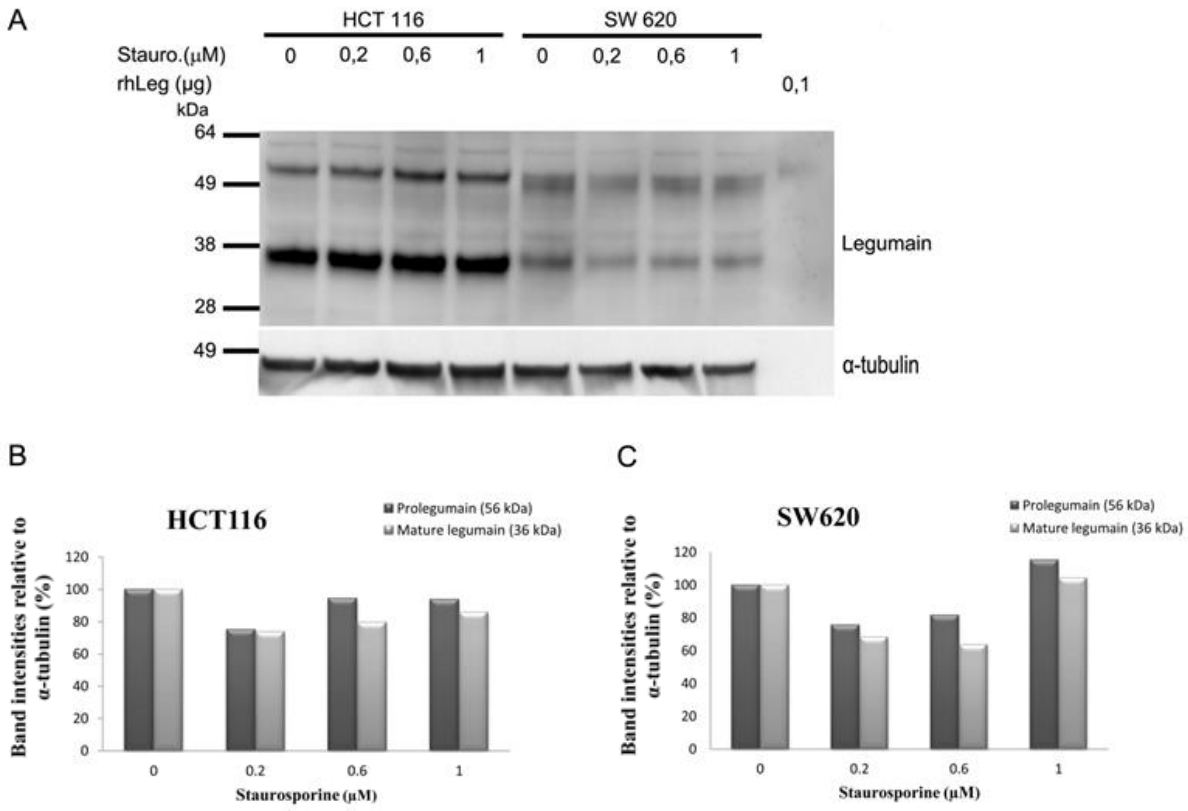

Figure 4.9: Legumain processing and expression in HCT116 and SW620 cells treated with staurosporine. (A) HCT116 and SW620 cells were treated with staurosporine for 0.5 hour using the indicated concentrations. The control cells were treated with 10 µl DMSO. Protein expression was analyzed by electrophoresis and immunoblotting. All lanes (except rhLeg) were loaded with 30 µg total protein. The filters were stained with a specific antibody against legumain (upper panel) and α- tubulin (lower panel) (n=1). Stauro; Staurosporine. (B and C) The graphs shows densitometry measurements (using GeneTools) of the immunoblots with prolegumain and mature legumain relative to loading control (α-tubulin) (n=1).

The experiment was further optimized using H7, a narrow spectrum protein kinase inhibitor. The intention, by utilizing a narrow spectrum inhibitor instead of staurosporine, was to obtain less adverse cellular processes and changes in the morphology. HCT116 and SW620 cells were treated with 0, 5, 15 or 30 µg/ml H7 for 1 hour (Grotterod *et al.*, 2010). Light microscopy of the cells demonstrated that, in contrast to staurosporine, H7 did not cause alterations in the cellular morphology (not shown). However, immunoblotting showed similar legumain expression and processing in control and treated cells, demonstrating that there were apparently no change in legumain expression patterns or molecular weight after treatment with H7 (Fig. 4.10 A), as reflected by total band intensities of legumain (Fig. 4.10 B and C)

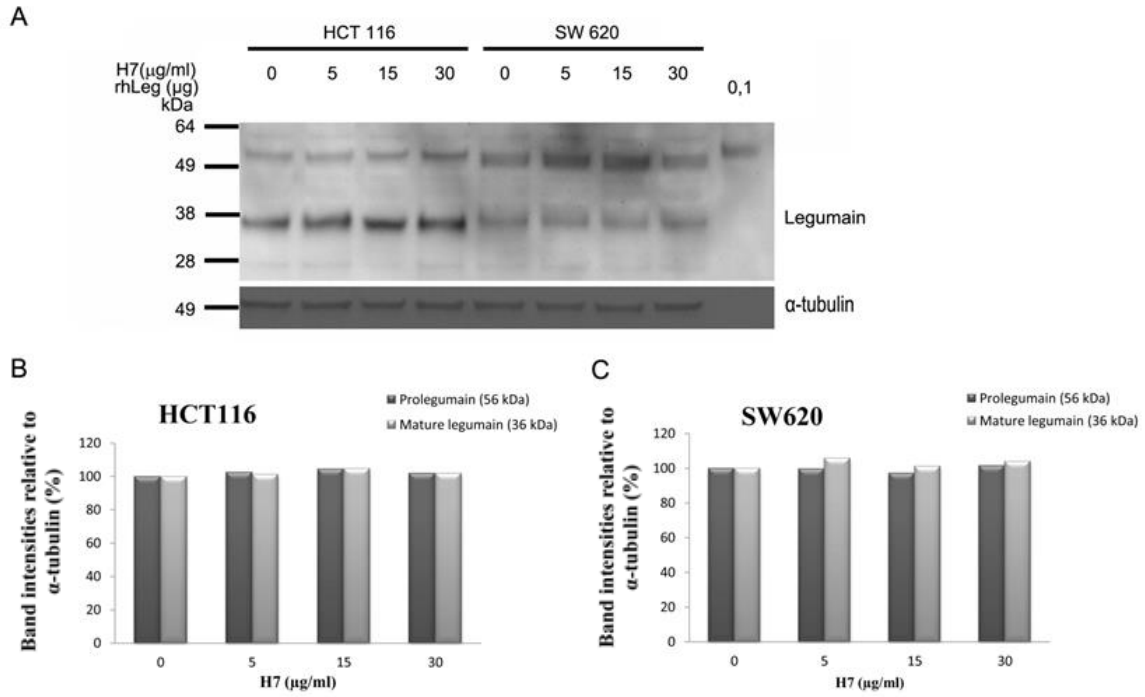

Figure 4.10: Legumain processing and expression in HCT116 and SW620 cells treated with H7. (A) HCT116 and SW620 cells were treated with H7 for 1 hour using the indicated concentrations. The control cells were treated with 10 µl ddH_20. Protein expression was analyzed by electrophoresis and immunoblotting. All lanes (except rhLeg) were loaded with 20 µg total protein. The filters were stained with a specific antibody against legumain (upper panel) and α- tubulin (lower panel) (n=1). (B and C) The graphs shows densitometry measurements (using GeneTools) of the immunoblots with prolegumain and mature legumain relative to loading control (α-tubulin) (n=1).

Together, these results demonstrate that inhibition of phosphorylation using either staurosporine or H7 did not seem to affect legumain expression or processing. Based on these initial data, it was chosen not to continue with experiments investigating further the implications of legumain phosphorylation.

5 Discussion

The cysteine proteinase legumain is overexpressed in many solid human tumors and have been associated with increased metastatic potential (Liu *et al.*, 2003). Metastasis is the major cause of cancer-related deaths, and constitutes a major problem for cancer therapy (Talmadge *et al.*, 2010). Cysteine proteinases (in particular legumain) are considered as promising candidates to be utilized for cancer specific prodrug targeting (Liu *et al.*, 2003). However, the lack of pre-established knowledge has led to failure in similar approaches (Turk, 2006). Currently, the knowledge about subcellular localization, trafficking and requirements for legumain activation remains largely unexplored. This needs to be revealed before legumain are to be utilized for therapeutic intervention. The present study was initiated to reveal the importance of legumain glycosylation and phosphorylation, two frequent modifications that have been found to play an important role in cellular trafficking and protein function (Farley *et al.*, 2009). In this present work we show that glycosylation is necessary for legumain maturation and nuclear transport. We also demonstrated that secretion of legumain is apparently independent of glycosylation. Additionally, it was demonstrated that manipulation of phosphorylation did not affect legumain expression or processing pattern.

5.1 The choice of cell lines

The two colorectal cell lines HCT116 and SW620 were used in this study. The choice of these cell lines can be explained by two main reasons. First, the cell lines have been found to express high levels of endogenous legumain. Second, a substantial difference in their relative amount of the pro- and active forms has been observed (Haugen *et al.*, 2013). SW620 express high levels of the proform and low levels of the mature form, while the opposite is the case for HCT116. Several explanations have been suggested for the differences in legumain processing, and thus proteolytic activity between these cell lines. Among other factors, it has been hypothesized that altered glycosylation may explain why SW620 exhibits overall less mature legumain (Haugen *et al.*, 2013).We observed similar mass shift from glycosylated to unglycosylated prolegumain in both cell lines following tunicamycin treatment, thus they both seem to be glycosylated. However, an eventual difference in composition of these glycosylations remains unexplained. Based on time and work limits, we chose to focus on HCT116 in most of our glycosylation experiments. Additionally, HCT116 cells have a larger

cytoplasm (previously observed by microscopy), making it more suitable for visualization and interpretation by use of immunofluorescence.

5.2 Legumain and glycosylation

Before initiating this study, presence of N-linked glycans on legumain was confirmed by our research group at the Department of Tumor Biology (Haugen *et al.*, unpublished data, as shown in chapter 1.8.2). The asparagine acceptors that are N-linked glycosylated are always present in the tripeptide sequence N-X-S/T, were X is any amino acid except proline (Pless *et al.*, 1977). In legumain, this specific sequence is present four times (Chen *et al.*, 1997). However, it has been demonstrated that this sequence alone is not sufficient for N-linked glycosylation. It seems likely that this tripeptide must be accessible in the protein conformation, and studies have revealed that approximately one third of the potential sites in proteins are actually glycosylated (Kornfeld *et al.*, 1985). Most recently, our research group identified that at least three out of the four potential glycosylation sites in legumain seem to be occupied (Haugen *et al.*, unpublished data, as shown in chapter 1.8.2). There are three main types of N-linked oligosaccharide that can be attached to the target protein termed high mannose, complex and hybrid. The three classes all share a common core, but differ in their outer chain (Kornfeld *et al.*, 1985, Shandala *et al.*, 2001). By immunoblotting, we found that both PNGase treatment and Endo H treatment explicit gave rise to identical shift of the apparent molecular mass from 56 to 47 kDa (proform) and from 36 to 28 kDa (mature form) of legumain. Thus, we identified that the N-glycans attached to legumain are of the high mannose or hybrid types.

5.2.1 The choice of N-linked glycosylation inhibitor

N-linked glycosylation is a complex process and involves sequential steps. There are various means of interfering with N-linked glycosylation, both in the early and the late stage. In this study tunicamycin was employed, a well-used biochemical tool. The advantage to utilize this tool was considered to be its specificity towards the common core region present in all N-linked glycans. Additionally, it was desirable to prevent glycosylation altogether rather than using compounds that cause alterations in the structure of the carbohydrate chain (Heifetz *et al.*, 1979, Elbein, 1987).

In the literature, the amount of tunicamycin described to prevent glycosylation varies between 0.1 - 10 µg/ml. However, the concentration that can be used is generally limited by its toxicity, and the cell line may differ in their susceptibility to this drug (Elbein, 1987). Therefore, an optimal concentration needs to be established for every cell line. In the cell lines HCT116 and SW620 used herein, a concentration of 5 µg/ml tunicamycin seemed to be an optimal concentration to inhibit glycosylation. This concentration was chosen on the basis of the observed effect on legumain glycosylation together with low cellular toxicity.

5.2.2 Effect of N-linked glycosylation on legumain expression, processing and localization

Two molecular forms of legumain were observed in HCT116 lysates treated with tunicamycin, and were identified as unglycosylated proform (47 kDa) and glycosylated mature form (36 kDa). Of particular interest, the unglycosylated mature form was not detected. First, we hypothesize that this might be due to duration of exposure. When employing tunicamycin *in vitro*, it takes a certain time to replace endogenous legumain with newly synthesized unglycosylated forms. Additionally, the inactive proenzyme (prolegumain) require a multistep processing to reach its mature form (Li *et al.*, 2003). Assuming that both of these processes were not completed after the time of exposure used in our experiments, we increased the treatment time from 24 to 48 hours. By increasing time of exposure, it also seemed reasonable to believe that the formation of the glycosylated mature form would disappear due to complete turnover of the initially glycosylated legumain.

However, by increasing the time of exposure in the HCT116 cell line the unglycosylated mature form was still not present. The lack of processing to the mature form resulted in an accumulation of the unglycosylated proform. This can partly be explained by the stability of legumain. Prolegumain is presumed to be highly stable, whereas mature legumain has a high turnover rate (Haugen, personal communication). Thus, when mature legumain is not formed, it may be hypothesized that this would lead to accumulation of the proform. Moreover, small amounts of the glycosylated mature form were still detected after prolonged tunicamycin exposure. It seemed as glycosylated legumain synthesized prior to treatment had a longer turnover rate than the longest time of exposure (48 hours) used in our experiments. However, a further increased tunicamycin exposure would not be favorable, as this presumably would cause several adverse cellular processes such as cell cycle arrest and apoptosis (Savage *et al.*,

1983, Elbein, 1987). The treatment time with tunicamycin was limited by its adverse effects. Thus, using this method we cannot determine whether a treatment time over 48 hours would lead to appearance of the unglycosylated mature form or turnover of endogenous legumain synthesized prior to treatment.

In our experiments, tunicamycin treatment resulted in an accumulation of the proform and no detectable mature form (described in previous section), suggesting that inhibition of glycosylation had affected the maturation process. We hypothesized that there were two explanations for the lack of processing to the unglycosylated mature form: (1) altered trafficking, in which unglycosylated prolegumain is not transported to the lysosomes; or (2) legumain is transported to the lysosomes, but not processed to the mature form when unglycosylated.

In the case of our first hypothesis; altered legumain trafficking. Several reports have suggested that glycosylation is important in the regulation of protein transport. Hemagglutinin, a well characterized viral glycoprotein, is one example where glycosylation constitute a key event regulating the transport out of the RER (Copeland *et al.*, 1986, Gallagher *et al.*, 1992). There are, however, also reports showing that glycoproteins can be transported out of the RER without being glycosylated. For instance fibronectin, which is normally glycosylated, although glycosylation is not necessary for secretion or the biological activity (Olden *et al.*, 1979, Copeland *et al.*, 1986). The dominant theory for intracellular transport of legumain after synthesis is through the Golgi network and further into lysosomes through the endosomes. It is assumed that glycosylation is important for transport to the lysosomes, which is also the main compartment where inactive prolegumain is thought to be processed into the active form of legumain (Chen et al., 2000, Ishidoh et al., 2002, Lecaille et al., 2004). Furthermore, the localization of legumain is not strictly lysosomal, it has also been observed in other subcellular compartments, such as extracellular and in the nucleus (Liu *et al.*, 2003, Haugen *et al.*, 2013). As observed in the HCT116 total lysates (Haugen *et al.*, unpublished data, as seen in chapter 1.8.2), secreted and nuclear localized legumain have also been found to be glycosylated (Haugen *et al.*, Dept. of Tumor Biology, Oslo University Hospital). However, it is not fully known whether and how glycosylation participates in the intracellular or extracellular transport of legumain.

Protein isolation from the intra-organelle membrane fraction of HCT116 cells showed presence of unglycosylated prolegumain, but not unglycosylated mature legumain. This is in

concurrence with the observation made in total cell lysates. However, the intramembranous fraction referred to in this study includes different vesicular structures in the protein transport chain, i.e. RER, Golgi, endosomes and the lysosomes. The intention was to study whether unglycosylated prolegumain is retrained in RER, Golgi or the endosomes on its route to the lysosomes. Therefore, it seemed necessary to utilize methods that separate compartments that constitute the intramembranous fraction. One possibility is to use biochemical techniques to separate Golgi (by the use of stepwise sucrose gradient centrifugations) from the other fractions, and subsequent separate the endosomes from the lysosomes (Sandvig *et al.*, 1991, Egeberg *et al.*, 2001) By use of this method we indeed tried to separate Golgi from the other intramembranous fractions of HCT116 cells (not shown), however, the results were not suitable to draw any conclusions. Another method that can give valuable information on subcellular localization is using immunofluorescence confocal microscopy. This was done to visualizing the distribution of unglycosylated legumain in early- and late endosomes/lysosomes. By confocal microscopy, we observed that unglycosylated legumain showed some colocalization with the lysosomes. However, this lysosomal localization needs to be supported by biochemical techniques, e.g. the aforementioned compartment separation methods, before we can establish evidence that the legumain glycosylation status is not important for transport to the lysosomes. In addition, colocalization of glycosylated legumain and the lysosomes in untreated HCT116 cells was surprisingly low, implying that the imaging techniques requires to be repeated and optimized using other antibodies

A highly interesting finding was the observed differences in nuclear legumain expression between tunicamycin-treated and untreated cells. In line with previous reports, glycosylated legumain was found to be highly expressed in the cell nucleus of HCT116 cells (Haugen *et al.*, 2013). However, after tunicamycin treatment, nuclear legumain was only present at a minor level. Thus, legumain transport into the nucleus seems to be dependent on glycosylation. However, how it gains access to the nucleus cannot be determined from these results. On the other hand, we showed that both glycosylated and unglycosylated legumain were secreted from HCT116 cells. This result indicates that secretion to the extracellular environment is apparently independent of glycosylation. It has recently been suggested that polyubiquitination of prolegumain promote extracellular secretion, and may regulate whether legumain are retrained in the cells or secreted to the environment (Lin *et al.*, 2014). Thus, it seems likely that glycosylation and ubiquitination do not influence legumain secretion in the

same way. However, detail knowledge concerning the secretory pathway of legumain will require further studies.

In the case of the other formed hypothesis; legumain is transported to the lysosomes, but not processed to the mature form when unglycosylated. Legumain is dependent on several events to reach its mature form, and it is proposed that lysosomal proteinases are taking part in the maturation process (Li *et al.*, 2003). Therefore, we speculate that proteinases only recognize and activate the glycosylated form of prolegumain. However, this hypothesis was not tested.

5.3 Legumain and phosphorylation

Preliminary data from our research group at the Department of Tumor Biology showed that legumain was susceptible to phosphorylation (Haugen *et al.*, unpublished data, shown in chapter 1.9.1). However, the positions of the phosphate groups or its function could not be interpreted from these results and needed to be further investigated.

5.3.1 The choice of kinase inhibitors

To study the role of phosphorylation, HCT1116 and SW620 cells were treated with staurosporine. The advantage to utilize this compound was considered to be its inhibitory activity towards a broad spectrum of protein kinases. However, we observed morphological changes following treatment, even when decreasing time of exposure. Staurosporine is widely used to induce apoptosis in a variety of cells. Thus, it seemed reasonable to believe that the observed morphological changes were due to apoptosis. As apoptosis itself may influence the interpretation of upcoming results, we optimized the experiment using the protein kinase inhibitor H7. H7 is more selective and staurosporine, and did not cause apoptosis in neither SW620 nor HC116 cells.

5.3.2 Effect of phosphorylation on legumain processing

Phosphorylation of proteins turns cellular signaling on and off, and has been shown to be important for protein activity (Farley *et al.*, 2009). Protein phosphorylation is catalyzed by protein kinases, which have emerged as promising targets used in the clinic (Cohen, 2002). By using a broad or narrow spectrum protein kinase inhibitor, we found that there were

apparently no variations in legumain processing between control and untreated cells. Thus, our experiments point towards that phosphorylation is not important for legumain processing.

5.4 Methodological considerations

To support our data, we chose to use both biochemical and imaging analysis techniques. Subcellular enrichment, immunoblotting and confocal microscopy are the techniques that have formed the basis of many of our results.

Subcellular enrichment is a biochemical technique which enables isolation and enrichment of proteins from different cellular compartments. It is a challenging method, and one important limitation is that total purity of the isolated fractions is practically unachievable. In this present work, we added washing steps to the protocol (see chapter 3.6) with the aim to limit the degree of contamination and to ensure high purity of each fraction. Additionally, compartment specific protein markers (proteins of presumed limited distribution) were used as purity control in the immunoblot analyses. We chose to utilize protein markers for the intramembranous fraction (ARSB) and the nucleus fraction (SP1), as these two fractions showed interesting results. The protein markers demonstrated that there were good enrichment and purity of the subcellular compartment.

Confocal microscopy is a well-used imaging technique to visualize different cellular components. In this present work we preformed double and triple staining and we spent much time trying to find the appropriate primary and secondary antibodies. First of all, multicolor staining requires that the primary antibodies have different host species and that the secondary antibodies recognize those species exclusively. Second, when using multicolor staining panels it is important to eliminate spectral overlap between the fluorochromes. To avoid spectral overlap, we utilized secondary antibodies conjugated with fluorochromes which exhibit largely separated emission spectra and tune the confocal detectors accordingly. Finally, it was also important to choose an appropriate concentration of each antibody. To low concentration can result in absent signal, and to high concentration may give rise to unspecific background signals. The utilized concentrations were based on the manufactures recommendations and experiences within our research group.

6 Conclusion

1) Glycosylation is necessary for legumain processing and activation.

2) Glycosylation is necessary for intracellular transport of legumain into the nucleus.

3) Legumain secretion to the extracellular environment is apparently independent of the glycosylation status.

4) Phosphorylation is apparently not important for legumain processing and activation.

7 Future perspectives

The limited time period of this project causes several questions to be left unanswered and further investigation and validation is necessary.

First of all, to confirm the results on the present project, more cell lines and analysis techniques needs to be tested. It would be of particular interest reveal the exact localization of unglycosylated legumain by both imaging and biochemical techniques. These results may give us some further answers to why mature legumain is not formed when the proteinase is unglycosylated, and elucidate how glycosylation is necessary for nuclear transport. Another important question that should be revealed is how legumain is secreted to the extracellular environment.

An important step would also be to measure legumain activity in HTC116 cells after tunicamycin treatment, and to characterize the carbohydrate groups on legumain by mass spectroscopy. Furthermore, it would be of interest to determine the position of phosphate groups on the legumain protein and to investigate the subcellular localization of legumain forms after cell treatment with protein kinase inhibitors.

References

Aebi, M. (2013). "N-linked protein glycosylation in the ER." Biochim Biophys Acta **1833**(11): 2430-2437.

Alvarez-Fernandez, M., A. J. Barrett, B. Gerhartz, P. M. Dando, J. Ni and M. Abrahamson (1999). "Inhibition of mammalian legumain by some cystatins is due to a novel second reactive site." J Biol Chem **274**(27): 19195-19203.

Apweiler, R., H. Hermjakob and N. Sharon (1999). "On the frequency of protein glycosylation, as deduced from analysis of the SWISS-PROT database." Biochim Biophys Acta **1473**(1): 4-8.

Bajjuri, K. M., Y. Liu, C. Liu and S. C. Sinha (2011). "The legumain protease-activated auristatin prodrugs suppress tumor growth and metastasis without toxicity." ChemMedChem **6**(1): 54-59.

Barrett, A. J. (2001). Proteases. Current Protocols in Protein Science, John Wiley & Sons, Inc.

Barrett, A. J., N. D. Rawlings, G. Salvesen and J. Fred Woessner (2013). Introduction. Handbook of Proteolytic Enzymes. N. D. Rawlings and G. Salvesen, Academic Press**:** li-liv.

Blom, N., S. Gammeltoft and S. Brunak (1999). "Sequence and structure-based prediction of eukaryotic protein phosphorylation sites." Journal of Molecular Biology **294**(5): 1351-1362.

Cancer Registry of Norway. (2011). "Cancer of Norway 2011." Retrieved 14.04.2014, from http://www.kreftregisteret.no/no/Generelt/Publikasjoner/Cancer-in-Norway/Cancer-in-Norway-2011/.

Chen, J.-M., P. M. Dando, N. D. Rawlings, M. A. Brown, N. E. Young, R. A. Stevens, E. Hewitt, C. Watts and A. J. Barrett (1997). "Cloning, Isolation, and Characterization of Mammalian Legumain, an Asparaginyl Endopeptidase." Journal of Biological Chemistry **272**(12): 8090-8098.

Chen, J. M., P. M. Dando, R. A. Stevens, M. Fortunato and A. J. Barrett (1998). "Cloning and expression of mouse legumain, a lysosomal endopeptidase." Biochem J **335 (Pt 1)**: 111-117.

Chen, J. M., M. Fortunato and A. J. Barrett (2000). "Activation of human prolegumain by cleavage at a C-terminal asparagine residue." Biochem J **352 Pt 2**: 327-334.

Chen, J. M., M. Fortunato, R. A. Stevens and A. J. Barrett (2001). "Activation of progelatinase A by mammalian legumain, a recently discovered cysteine proteinase." Biol Chem **382**(5): 777-783.

Choi, K. Y., M. Swierczewska, S. Lee and X. Chen (2012). "Protease-activated drug development." Theranostics **2**(2): 156-178.

Choi, S. J., S. V. Reddy, R. D. Devlin, C. Menaa, H. Chung, B. F. Boyce and G. D. Roodman (1999). "Identification of Human Asparaginyl Endopeptidase (Legumain) as an Inhibitor of Osteoclast Formation and Bone Resorption." Journal of Biological Chemistry **274**(39): 27747-27753.

Chwieralski, C. E., T. Welte and F. Bühling (2006). "Cathepsin-regulated apoptosis." Apoptosis **11**(2): 143-149.

Clerin, V., H. H. Shih, N. Deng, G. Hebert, C. Resmini, K. M. Shields, J. L. Feldman, A. Winkler, L. Albert, V. Maganti, A. Wong, J. E. Paulsen, J. C. Keith, Jr., G. P. Vlasuk and D. D. Pittman (2008). "Expression of the cysteine protease legumain in vascular lesions and functional implications in atherogenesis." Atherosclerosis **201**(1): 53-66.

Cohen, P. (2001). "The role of protein phosphorylation in human health and disease. The Sir Hans Krebs Medal Lecture." Eur J Biochem **268**(19): 5001-5010.

Cohen, P. (2002). "Protein kinases-the major drug targets of the twenty-first century?" Nat Rev Drug Discov **1**(4): 309-315.

Copeland, C. S., R. W. Doms, E. M. Bolzau, R. G. Webster and A. Helenius (1986). "Assembly of influenza hemagglutinin trimers and its role in intracellular transport." J Cell Biol **103**(4): 1179-1191.

Dando, P. M., M. Fortunato, L. Smith, C. G. Knight, J. E. McKendrick and A. J. Barrett (1999). "Pig kidney legumain: an asparaginyl endopeptidase with restricted specificity." Biochem J **339 (Pt 3)**: 743-749.

Egeberg, M., R. Kjeken, S. O. Kolset, T. Berg and K. Prydz (2001). "Internalization and stepwise degradation of heparan sulfate proteoglycans in rat hepatocytes." Biochim Biophys Acta **1541**(3): 135-149.

Elbein, A. D. (1987). "Inhibitors of the biosynthesis and processing of N-linked oligosaccharide chains." Annu Rev Biochem **56**: 497-534.

Farley, A. R. and A. J. Link (2009). Chapter 40 Identification and Quantification of Protein Posttranslational Modifications. Methods in Enzymology. R. B. Richard and P. D. Murray, Academic Press. **Volume 463:** 725-763.

Ferlay, J., H. R. Shin, F. Bray, D. Forman, C. Mathers and D. M. Parkin (2010). "Estimates of worldwide burden of cancer in 2008: GLOBOCAN 2008." Int J Cancer **127**(12): 2893-2917.

Frayling, I. M. (2001). Colorectal Cancer: Genetics. eLS, John Wiley & Sons, Ltd.

Gallagher, P. J., J. M. Henneberry, J. F. Sambrook and M. J. Gething (1992). "Glycosylation requirements for intracellular transport and function of the hemagglutinin of influenza virus." J Virol **66**(12): 7136-7145.

Graves, J. D. and E. G. Krebs (1999). "Protein phosphorylation and signal transduction." Pharmacol Ther **82**(2-3): 111-121.

Grotterod, I., G. M. Maelandsmo and K. Boye (2010). "Signal transduction mechanisms involved in S100A4-induced activation of the transcription factor NF-kappaB." BMC Cancer **10**: 241.

Halfon, S., S. Patel, F. Vega, S. Zurawski and G. Zurawski (1998). "Autocatalytic activation of human legumain at aspartic acid residues." FEBS Letters **438**(1–2): 114-118.

Hanahan, D. and R. A. Weinberg (2011). "Hallmarks of cancer: the next generation." Cell **144**(5): 646-674.

Hanks, S. K. (1991). "Eukaryotic protein kinases." Current Opinion in Structural Biology **1**(3): 369-383.

Hanks, S. K. and T. Hunter (1995). "Protein kinases 6. The eukaryotic protein kinase superfamily: kinase (catalytic) domain structure and classification." FASEB J **9**(8): 576-596.

Haugen, M. H., H. T. Johansen, S. J. Pettersen, R. Solberg, K. Brix, K. Flatmark and G. M. Maelandsmo (2013). "Nuclear Legumain Activity in Colorectal Cancer." PLoS ONE **8**(1): e52980.

Heifetz, A., R. W. Keenan and A. D. Elbein (1979). "Mechanism of action of tunicamycin on the UDP-GlcNAc:dolichyl-phosphate Glc-NAc-1-phosphate transferase." Biochemistry **18**(11): 2186-2192.

Hidaka, H., M. Inagaki, S. Kawamoto and Y. Sasaki (1984). "Isoquinolinesulfonamides, novel and potent inhibitors of cyclic nucleotide dependent protein kinase and protein kinase C." Biochemistry **23**(21): 5036-5041.

Hunter, T. (1989). "Protein modification: phosphorylation on tyrosine residues." Curr Opin Cell Biol **1**(6): 1168-1181.

Huttunen, K. M., H. Raunio and J. Rautio (2011). "Prodrugs--from serendipity to rational design." Pharmacol Rev **63**(3): 750-771.

Ishidoh, K. and E. Kominami (2002). "Processing and activation of lysosomal proteinases." Biol Chem **383**(12): 1827-1831.

Katz, J., J. E. Janik and A. Younes (2011). "Brentuximab Vedotin (SGN-35)." Clinical Cancer Research **17**(20): 6428-6436.

Kornfeld, R. and S. Kornfeld (1985). "Assembly of asparagine-linked oligosaccharides." Annu Rev Biochem **54**: 631-664.

Krebs, E. G. and J. A. Beavo (1979). "Phosphorylation-dephosphorylation of enzymes." Annu Rev Biochem **48**: 923-959.

Kuhn, P., A. L. Tarentino, T. H. Plummer Jr and P. Van Roey (1994). "Crystallization and Preliminary Crystallographic Analysis of Peptide-N4-(N-acetyl-β-d-glucosaminyl)asparagine Amidase PNGase F." Journal of Molecular Biology **241**(4): 622-623.

Lecaille, F., D. Muno, E. Kominami and K. Ishidoh (2004). "Proteinases participating in the processing and activation of prolegumain in primary cultured rat macrophages." Biol Chem **385**(6): 511-516.

Lehle, L. and W. Tanner (1976). "The specific site of tunicamycin inhibition in the formation of dolichol-bound N-acetylglucosamine derivatives." FEBS Lett **72**(1): 167-170.

Li, D. N., S. P. Matthews, A. N. Antoniou, D. Mazzeo and C. Watts (2003). "Multistep Autoactivation of Asparaginyl Endopeptidase in Vitro and in Vivo." Journal of Biological Chemistry **278**(40): 38980-38990.

Lin, Y., Y. Qiu, C. Xu, Q. Liu, B. Peng, G. F. Kaufmann, X. Chen, B. Lan, C. Wei, D. Lu, Y. Zhang, Y. Guo, Z. Lu, B. Jiang, T. S. Edgington and F. Guo (2014). "Functional Role of Asparaginyl Endopeptidase Ubiquitination by TRAF6 in Tumor Invasion and Metastasis." J Natl Cancer Inst **106**(4): dju012.

Liu, C., C. Sun, H. Huang, K. Janda and T. Edgington (2003). "Overexpression of legumain in tumors is significant for invasion/metastasis and a candidate enzymatic target for prodrug therapy." Cancer Res **63**(11): 2957-2964.

Liu, Y., K. M. Bajjuri, C. Liu and S. C. Sinha (2012). "Targeting cell surface alpha(v)beta(3) integrin increases therapeutic efficacies of a legumain protease-activated auristatin prodrug." Mol Pharm **9**(1): 168-175.

Liu, Z., S. W. Jang, X. Liu, D. Cheng, J. Peng, M. Yepes, X. J. Li, S. Matthews, C. Watts, M. Asano, I. Hara-Nishimura, H. R. Luo and K. Ye (2008). "Neuroprotective actions of PIKE-L by inhibition of SET proteolytic degradation by asparagine endopeptidase." Mol Cell **29**(6): 665-678.

López-Otín, C. and J. S. Bond (2008). "Proteases: Multifunctional Enzymes in Life and Disease." Journal of Biological Chemistry **283**(45): 30433-30437.

Lynch, H. T. and A. de la Chapelle (2003). "Hereditary colorectal cancer." N Engl J Med **348**(10): 919-932.

Mahato, R., W. Tai and K. Cheng (2011). "Prodrugs for improving tumor targetability and efficiency." Adv Drug Deliv Rev **63**(8): 659-670.

Manoury, B., E. W. Hewitt, N. Morrice, P. M. Dando, A. J. Barrett and C. Watts (1998). "An asparaginyl endopeptidase processes a microbial antigen for class II MHC presentation." Nature **396**(6712): 695-699.

Murthy, R. V., G. Arbman, J. Gao, G. D. Roodman and X.-F. Sun (2005). "Legumain Expression in Relation to Clinicopathologic and Biological Variables in Colorectal Cancer." Clinical Cancer Research **11**(6): 2293-2299.

Norwegian Electronic Legehåndbok. (2014). "Cancer." Retrieved 15.04.2014, from http://legehandboka.no/kreft/pasientinformasjon/om-kreft/kreft-1808.html.

O'Neill, R. A. (1996). "Enzymatic release of oligosaccharides from glycoproteins for chromatographic and electrophoretic analysis." Journal of Chromatography A **720**(1–2): 201-215.

Ohtsubo, K. and J. D. Marth (2006). "Glycosylation in cellular mechanisms of health and disease." Cell **126**(5): 855-867.

Olden, K., R. M. Pratt and K. M. Yamada (1979). "Role of carbohydrate in biological function of the adhesive glycoprotein fibronectin." Proc Natl Acad Sci U S A **76**(7): 3343-3347.

Omura, S., Y. Iwai, A. Hirano, A. Nakagawa, J. Awaya, H. Tsuchya, Y. Takahashi and R. Masuma (1977). "A new alkaloid AM-2282 OF Streptomyces origin. Taxonomy, fermentation, isolation and preliminary characterization." J Antibiot (Tokyo) **30**(4): 275-282.

Pless, D. D. and W. J. Lennarz (1977). "Enzymatic conversion of proteins to glycoproteins." Proc Natl Acad Sci U S A **74**(1): 134-138.

Powell, L. D. (2001). "Inhibition of N-linked glycosylation." Curr Protoc Immunol **Chapter 8**: Unit 8 14.

Rawlings, N. D., M. Waller, A. J. Barrett and A. Bateman (2014). "MEROPS: the database of proteolytic enzymes, their substrates and inhibitors." Nucleic Acids Res **42**(Database issue): D503-509.

Ruegg, U. T. and G. M. Burgess (1989). "Staurosporine, K-252 and UCN-01: potent but nonspecific inhibitors of protein kinases." Trends Pharmacol Sci **10**(6): 218-220.

Sandvig, K., K. Prydz, S. H. Hansen and B. van Deurs (1991). "Ricin transport in brefeldin A-treated cells: correlation between Golgi structure and toxic effect." J Cell Biol **115**(4): 971-981.

Savage, K. E. and P. S. Baur (1983). "Effect of tunicamycin, an inhibitor of protein glycosylation, on division of tumour cells in vitro." J Cell Sci **64**: 295-306.

Sepulveda, F. E., S. Maschalidi, R. Colisson, L. Heslop, C. Ghirelli, E. Sakka, A. M. Lennon-Dumenil, S. Amigorena, L. Cabanie and B. Manoury (2009). "Critical role for asparagine endopeptidase in endocytic Toll-like receptor signaling in dendritic cells." Immunity **31**(5): 737-748.

Shandala, T., E. J. Parkinson-Lawrence and D. A. Brooks (2001). Protein: Cotranslational and Posttranslational Modification in Organelles. eLS, John Wiley & Sons, Ltd.

Shirahama-Noda, K., A. Yamamoto, K. Sugihara, N. Hashimoto, M. Asano, M. Nishimura and I. Hara-Nishimura (2003). "Biosynthetic Processing of Cathepsins and Lysosomal Degradation Are Abolished in Asparaginyl Endopeptidase-deficient Mice." Journal of Biological Chemistry **278**(35): 33194-33199.

Sparbier, K., S. Koch, I. Kessler, T. Wenzel and M. Kostrzewa (2005). "Selective isolation of glycoproteins and glycopeptides for MALDI-TOF MS detection supported by magnetic particles." J Biomol Tech **16**(4): 407-413.

Takatsuki, A., K. Arima and G. Tamura (1971). "Tunicamycin, a new antibiotic. I. Isolation and characterization of tunicamycin." J Antibiot (Tokyo) **24**(4): 215-223.

Talmadge, J. E. and I. J. Fidler (2010). "AACR centennial series: the biology of cancer metastasis: historical perspective." Cancer Res **70**(14): 5649-5669.

Tamaoki, T., H. Nomoto, I. Takahashi, Y. Kato, M. Morimoto and F. Tomita (1986). "Staurosporine, a potent inhibitor of phospholipid/Ca++dependent protein kinase." Biochem Biophys Res Commun **135**(2): 397-402.

Tkacz, J. S. and O. Lampen (1975). "Tunicamycin inhibition of polyisoprenyl N-acetylglucosaminyl pyrophosphate formation in calf-liver microsomes." Biochem Biophys Res Commun **65**(1): 248-257.

Turk, B. (2006). "Targeting proteases: successes, failures and future prospects." Nat Rev Drug Discov **5**(9): 785-799.

Valastyan, S. and Robert A. Weinberg (2011). "Tumor Metastasis: Molecular Insights and Evolving Paradigms." Cell **147**(2): 275-292.

Weitz, J., M. Koch, J. Debus, T. Hohler, P. R. Galle and M. W. Buchler (2005). "Colorectal cancer." Lancet **365**(9454): 153-165.

White, F. M. (2008). "Quantitative phosphoproteomic analysis of signaling network dynamics." Curr Opin Biotechnol **19**(4): 404-409.

Yeatman, T. J. (2001). Colon Cancer. eLS, John Wiley & Sons, Ltd.

Zafar, S., A. Nasir and H. Bokhari (2011). "Computational analysis reveals abundance of potential glycoproteins in Archaea, Bacteria and Eukarya." Bioinformation **6**(9): 352-355.

Zhang, B. F., F. F. Peng, J. Z. Zhang and D. C. Wu (2003). "Staurosporine induces apoptosis in NG108-15 cells." Acta Pharmacol Sin **24**(7): 663-669.

Zhao, L., T. Hua, C. Crowley, H. Ru, X. Ni, N. Shaw, L. Jiao, W. Ding, L. Qu, L. W. Hung, W. Huang, L. Liu, K. Ye, S. Ouyang, G. Cheng and Z. J. Liu (2014). "Structural analysis of asparaginyl endopeptidase reveals the activation mechanism and a reversible intermediate maturation stage." Cell Res **24**(3): 344-358.

Appendix

This appendix contains examples and formulas for solutions used in this master thesis.

1. Cell culture

1.1 Freezing medium

For 50 ml freezing medium:
35 ml Roswell Park Memorial Institute medium (RPMI) 1640 (Sigma-Aldrich)
10 ml FBS (which constitute 20 % of the final volume)
5 ml DMSO (which constitute 10 % of the final volume)

1.2 Growth medium (with and without FBS)

500 ml RPMI 1640
10 ml Hepes (1 M) (BioWittaker)
5 ml Glutamax (200 mM) (Invitrogen)
50 ml FBS

2. Harvesting

2.1 Lysis buffer (5X)

For 50 ml lysis buffer:
1.5 ml NaCl (5 M)
5 ml Tris-HCl pH 7.5 (0.5 M)
50 µl NP-40 (0.1 %)

2.2 Lysis buffer (1X) (Working solution)

0.5 ml lysis buffer (5X)
0.250 ml Completemini, Proteases inhibitor cocktail (Roche Diagnostics)
0.250 ml Phosstop, Phosphatase Inhibitor cocktail (Roche Diagnostics)
1.5 ml H_20 (Aqua Braun)

3. Immunoblotting (Westernblotting)

3.1 MES buffer

50 ml MES (20X) (Invitrogen)
950 ml ddH20

3.2 Transfer buffer

3 g Tris-HCl pH 7.5 (50 mM) (Merck)
14.4 g Glycine (Merck)
200 ml Methanol
Ad 1000 ml ddH20

3.3 TBST-buffer
20 ml Tris-HCl pH 7.5 (1 M) (Life technologies)
30 ml NaCl (5 M)
5 ml Tween 20 (20%) (Merck)
Ad 1000 ml ddH_2O

4. Indirect immunofluorescence

4.1 Hepes (200 mM)
10 ml Hepes (1 M)
40 ml pure H_20

4.2 Paraformaldehyde (PFA) (4 %)
0.5 ml PFA (8 %)
0.5 ml Hepes (200 mM)

4.3 Horse serum (HS) (3 %)
1 ml HS (100 %)
32.3 ml PBS (1X)

4.4 HS (0.1 %)
3.3 ml HS (0.3 %)
96.7 ml PBS (1X)

4.4 Triton- X100 (10 %)
2 ml Triton- X100 (100%)
18 ml PBS (1X)

4.5 Triton- X100 (2 %) (Working solution)
0.8 ml Triton- X100 (10 %)
39.2 ml PBS (1X)